NASA Contractor Report 167853

Investigation of Soot and Carbon Formation in Small Gas Turbine Combustors

T.J. Rosfjord

UNITED TECHNOLOGIES RESEARCH CENTER
East Hartford, CT 06108

April 1982

NASA
National Aeronautics and Space Administration

Lewis Research Center
Cleveland, Ohio 44135

NASA Contractor Report 167853

Investigation of Soot and Carbon Formation in Small Gas Turbine Combustors

T.J. Rosfjord

UNITED TECHNOLOGIES RESEARCH CENTER
East Hartford, CT 06108

April 1982

National Aeronautics and
Space Administration

Lewis Research Center
Cleveland, Ohio 44135

ACKNOWLEDGEMENTS

This report covers the investigation performed by United Technologies Research Center under NASA Contract NAS3-22524. The program was executed under the supervision of Mr. Daniel Briehl, the NASA Program Manager. The UTRC Principal Investigator was Dr. Thomas Rosfjord, who was greatly assisted by UTRC personnel including Dr. John McVey and Mr. Ralph Aiello. Pratt & Whitney Aircraft of Canada played a vital role in the program and the contributions of Messrs. Frank Shum and Maurice Weinberg were greatly appreciated.

Investigation of Soot and Carbon Formation in Small Gas Turbine Combustors

TABLE OF CONTENTS

LIST OF TABLES

LIST OF FIGURES

SUMMARY

An experimental program to investigate hardware configurations which attempt to minimize carbon formation and soot production without sacrificing performance in small gas turbine combustors has been conducted at the United Technologies Research Center. Four fuel injectors, embodying either airblast atomization, pressure atomization, or fuel vaporization techniques, were combined with nozzle air swirlers and injector sheaths, and evaluated at test conditions which included and extended beyond standard small gas turbine combustor operation. The testing was conducted in three phases. In the initial phase, eight configurations were screened at both sea-level-takeoff and idle test conditions in an attempt to identify the two most promising (low soot and carbon deposit) designs. The second phase of testing focused on the selected configurations in an attempt to quantify the influence of combustor pressure, inlet temperature, primary zone operation and combustor loading on soot and carbon formation. The third phase, a cycle test, which included specified time periods at idle, sea-level takeoff and cruise test conditions, was performed to simulate deposit formation during engine operation. The cycle test was performed with both Jet A and ERBS fuel.

Extensive testing was accomplished with configurations embodying either a spill return or a T-vaporizer injector; the unacceptable operation of configurations based on a splash-cone airblast or a bar-vaporizer injector prohibited performance characterization. Minimal carbon deposits were observed after tests using the spill return nozzle for either Jet A or ERBS test fuel. A more extensive film of soft carbon was observed on the vaporizer after operation at standard engine conditions, with carbonaceous growths forming on the device during off-design operation at low combustor inlet temperature. No deposits were observed on the combustor liner for either nozzle.

Test results indicated that smoke emission levels depended on the combustor fluid mechanics (especially the mixing rates near the injector), the atomization quality of the injector and the fuel hydrogen content. Reduced smoke emissions were attained by employing swirl to enhance the fuel-air mixing rates near the spill return nozzle. It appeared that excessive airflow across the nozzle face could compromise this process; lower smoke numbers were achieved for the smaller of two nozzle/sheath gaps investigated. Alternatively, the fuel-air premixing which occurred in the vaporizer injector promoted the lowest smoke numbers, with SN < 5 achieved at idle conditions. A rapid increase of exhaust smoke was observed for both the spill return and T-vaporizer nozzles as the inlet air temperature was reduced. This result was attributed to both reduced soot oxidation within the burner and altered mixing patterns at the reduced reference velocities. Higher combustor pressures also promoted smoke levels apparently because of an accelerated soot formation mechanism. In contrast, minimal smoke levels were attained at high combustor loadings because of the finer atomization achieved at higher fuel flow rates and enhanced gross mixing rates for elevated liner pressure losses. Tests with ERBS fuel resulted in smoke levels approximately twice the levels achieved with Jet A fuel.

Investigation of Soot and Carbon Formation in Small Gas Turbine Combustors

SECTION I - INTRODUCTION

Small gas turbine engines play an important role in aviation propulsion. They are a common powerplant for helicopters and small commercial carriers, and are rapidly gaining usage in the areas of twin-engine business aircraft, target-drone/RPV devices and long range missiles. A recent, NASA-sponsored study (Ref. 1) expounded upon these accomplishments of small gas turbine engines and projected an attractive growth potential into single and small twin-engine general aviation aircraft. It was noted that accompanying this growth will likely be demands for more fuel efficient and flexible engines with reduced maintenance demands. For example, many helicopters are used to ferry individuals to off-shore sites such as oil drilling platforms. Hence, attaining reliable, durable engines is the prime concern. On the other hand, fuel economy is critical for commuter aircraft applications, but fuel flexibility is more important to agricultural aircraft applications where high quality aviation fuel may not always be available.

Meeting such varied demands, as well as those associated with expected growth trends in the engine operating envelope, will require additional investigation and development of small gas turbine engine components. In particular, advances in combustor hardware ought be sought. While the demands on small engine combustors are similar to those imposed on large devices, the severity of many problems associated with meeting these demands is greater for small powerplants. For example, standard manufacturing tolerances become more significant as the components are scaled down, an aspect which could be important in fuel injection quality. Additionally, many small gas turbine engines employ compact, reverse flow annular combustors. Such devices have relatively high surface-to-volume ratios which can accentuate liner cooling/durability problems and place greater demands on fuel injection and distribution to achieve acceptable exhaust emissions (gaseous and particulate) and exit temperature pattern factor. Among the consequences of changes in either the engine operating envelope or fuel quality is an increased likelihood for the formation of carbon deposits within the combustor or the generation of higher concentrations of soot in the exhaust stream.

The processes leading to carbon deposition are not well defined. There is a controversy as to whether the origin of the carbon is basically different than the gas-phase reactions leading to nucleation and growth of soot particles. Furthermore, it is not clear whether the surface nucleation sites are created by adsorption of saturated molecules or are captured by the surface from the gas phase. It would be expected that the deposition process would generally be accelerated by high fuel concentrations near a surface, and certainly aggravated

by fuel wetting on either the combustor liner or the fuel nozzle. Excessive deposit growth on the liner could interfere with the cooling airflow, resulting in metal temperatures higher than the design limit. In addition, large deposits could break away from the surface and result in turbine blade damage. Carbon deposits on the fuel injector can affect the fuel spray quality, adversely altering the spray pattern. In addition to degrading combustor performance, catastrophic changes in either the exit temperature distribution or liner heat loading because of high temperature streaks could result.

The formation of soot, with the subsequent production of exhaust smoke, depends upon the local fuel-air stoichiometry, gas temperature and pressure, and the fuel properties. Inadequate fuel-air mixing can result in high soot loadings with subsequent high radiative heat transfer to the combustor liner. This consequence could particularly be aggravated by use of fuels with a hydrogen/carbon ratio lower than available in current fuels. Increased soot formation with the associated increased radiative heat transfer to the liner could result, placing even greater demands on burner designs with acute liner cooling problems. High soot concentrations in the exhaust stream will also result in a more visible exhaust plume, a generally undesirable feature for both commercial and military engine applications.

Carbon deposition and soot formation do not always occur together. That is, configurations which are prone to carbon deposition do not necessarily result in high exhaust smoke levels. Both of these phenomena, however, can be associated with the fuel injection process. Hence, it is appropriate to investigate fuel injector configurations and evaluate their tendency to avoid carbon deposition or soot formation while promoting the desirable operating characteristics of high combustion efficiency, low exit temperature pattern factor, ease of ignition, etc.

The United Technologies Research Center (UTRC) under contract to NASA-Lewis Research Center (NAS3-22524) has conducted an experimental program aimed at evaluating several fuel nozzle, air swirler, and shroud combinations with the goal of identifying configurations which result in low smoke and low carbon deposition operation. Pratt & Whitney Aircraft of Canada (PWC), a subsidiary of United Technologies Corporation, designed the combustor test rig and the injector swirler/shroud hardware. Four fuel injector concepts were investigated: a splash-cone airblast nozzle, a spill-return pressure atomizing nozzle, and two vaporizing nozzles. The testing was conducted in three phases. In Phase I, eight configurations were screened at idle and sea level takeoff (SLTO) test conditions corresponding to a JT15D gas turbine combustor. The two more promising configurations were further evaluated in Phase II by investigating the influence of changing combustor pressure, primary zone equivalence ratio, inlet air temperature, and combustor loading. The most promising configuration was evaluated in Phase III using a modified landing-takeoff cycle in an attempt to evaluate carbon deposition rates as might be experienced in an operational

engine. The Phase I and II investigations used Jet A fuel. Cycle tests were performed (Phase III) with Jet A and ERBS fuel. Section II of this report describes the fuel injection configurations investigated in this program, with the test facility and instrumentation detailed in Section III. The test results are presented in Section IV, summarized in Section V, with the program conclusions stated in Section VI.

SECTION II - TEST HARDWARE

The experimental program was conducted using a 60-deg sector of a JT15D annular combustor. Details of the model combustor and of the several fuel injection configurations are given in this section of the report.

Combustor Model

In an attempt to evaluate the several fuel injection configurations described below in a realistic small gas turbine combustor environment, a combustor model based on an existing engine was assembled. Pratt & Whitney Aircraft of Canada (PWC) produces a 11 kN thrust gas turbine for the commercial turbojet market. One version of this engine, the JT15D-4, was used as the basis for the combustor model. This engine utilizes a reversed flow, annular combustor with an annulus height of approximately 6 cm. The full engine contains twelve pressure atomizing fuel injectors. Two of the fuel injectors to be investigated were specified and supplied to UTRC by NASA (see below). The scale and geometry of the JT15D combustor, and the range of typical operating conditions indicated in Table 1, were well suited to these two injectors. The third nozzle was designed by PWC to be compatible with this combustor.

The model combustor was a 60-deg sector of the JT15D annular burner; it included a two-nozzle segment of the combustor liner (Figs. 1 and 2). The stainless steel weldment which held the combustor liner represented the inner and outer case walls. It had removable, water cooled sidewalls to aid in liner inspection or replacement and contained access ports in the head bulkhead to insert the fuel nozzles. A standard aircraft ignitor plug was mounted in one sidewall. The length of the straight transition duct provided a flow residence time equal to that experienced in an engine installation. A 30 percent open area perforated plate was positioned across the model inlet to promote a uniform distribution of the airflow. A remotely actuated airflow deflector was incorporated in the model to control the percentage of liner airflow which entered the combustor primary zone. This baffle was traversed within a contoured housing in the outer case wall. When positioned in the central region of the housing, the baffle imposed minimal liner flow pressure drop, resulting in a relatively fuel-lean primary zone. When positioned in an extreme position (either aft or forward), the baffle imposed a significant pressure drop (approximately 2 percent of the liner pressure), reducing the primary zone airflow. The actual airflow distribution was calculated from measurements of both the baffle and liner pressure losses and knowledge of the liner open-area distribution. Variations in primary zone equivalence ratios of from 0.95 to 1.1 could be experienced. A chain drive actuator positioned the baffle; a multiturn potentiometer indicated its relative location. Linear roller bushings guided the baffle support rods; close fabrication tolerances and use of a universal joint in the drive rod resulted in a smoothly actuating device.

The combustor model was contained in a section of nominal 50-cm pipe which acted as a plenum for the inlet airflow (Fig. 3). This commercial pipe vessel provided the necessary high pressure containment, eliminating the need to design and fabricate high strength, specially-contoured wall segments. The vessel contained sufficient penetrations to route fuel, sidewall coolant, ignition and instrumentation lines. It also contained a 15-cm dia. port opposite each model sidewall. These ports provided access to a plug in each sidewall which could be removed to allow inspection of the liner and nozzles by use of a borescope.

Fuel Injection Configurations

Four fuel injectors were investigated in this program. Two devices were specified and supplied by NASA--a splash-cone airblast injector and a spill-return pressure atomizing injector. Two nozzles embodying the vaporizer concept were designed by PWC. These four devices and the nozzle air swirler and shroud hardware designed for use with them are described in the sections below.

Splash Cone Airblast Injector

A splash cone injector was one of two nozzles specified and supplied by NASA (Fig. 4). The injector is an airblast device which uses an airflow accelerated by the liner pressure drop to shear fuel from the liquid sheet supposedly formed on the concave surface of the injector cone. The nozzle characteristics were determined in a previous NASA study (Ref. 2). The nozzle flow number was 6.4 ($PPH/PSID^{0.5}$), sufficiently high to avoid excessive fuel delivery pressures for JT15D conditions. The observed spray pattern was not uniform, however, but highly concentrated in four lobes, one opposite each of the injection orifices. The reported cone angle was 200 deg for most flowrates with spray Sauter mean diameters of 150 micrometers at high flow rates, increasing to 350 micrometers at low flowrates. While these general characteristics were also observed in spray booth tests performed at UTRC, they were not consistent from one nozzle to another. Jets of fuel were observed from some nozzle orifices, while others were apparently fully blocked. Fine wires were used to open each orifice, with two relatively well-matched devices selected for the combustor tests.

The generally poor atomizing characteristics of this injector posed a significant challenge to the design of nozzle swirler/shroud devices. Two approaches were adopted. The first, designated a partial swirl configuration (Fig. 5a) utilized concentric rings of non-swirled and 30-deg-swirled airflow in an attempt to aerodynamically contain the high cone-angle sprays. The swirl, non-swirl sequence was selected to introduce a second high shear-stress interface attempting to promote secondary atomization and fuel-air mixing. The

second configuration, designated a filming configuration (Fig. 5b) allowed the fuel to impinge on a venturi tube surrounding the injector, with the resulting fuel film being atomized by the inner and outer shear flows. Hence, in this configuration, the injector was to be used primarily to distribute the fuel on the venturi tube. As explained in Section IV, tests were performed only with the filming configuration.

Spill-Return Injector

A spill-return injector was the second of the two nozzles specified and supplied by NASA (Fig. 6). The injector is similar to a conventional pressure-atomizing device which relies upon a high tangential fuel velocity in the spin chamber upstream of the nozzle orifice to achieve high levels of atomization. In the conventional pressure atomizer design, atomization quality degrades with reduced fuel flowrate because of lower spin velocities. In a spill return device, a portion of the flowrate delivered to the spin chamber is returned to the source. Hence high tangential velocities (and high atomization quality) can be retained for reduced combustor fuel flows. The nozzle characteristics were determined in a previous NASA study (Ref. 2). The nozzle flow number was 3.1 ($PPH/PSID^{0.5}$), a value lower than desired for a JT15D requirement. That is, fuel pressures up to 10 MPa were required to deliver a fuel flowrate corresponding to an SLTO test condition. A well-defined, hollow-cone spray was observed with a cone angle of 90 deg at high flowrates increasing to approximately 120 deg at low (idle) flowrates. Spray Sauter mean diameters of 100 micrometers were reported for most flowrates, decreasing to 75 micrometers at the maximum flow. The nozzles received by UTRC displayed high quality characteristics; the four nozzles received were equally matched to within 3 percent.

The JT15D engine uses a pressure atomizer as the bill-of-materials (BOM) injector. Hence, nozzle/swirler/shroud configurations emphasized use of hardware developed for JT15D use. Two basic configurations are depicted in Fig. 7. The non-swirl sheath is the JT15D BOM device, while the swirler device resulted from investigations of a low-emission JT15D configuration. The two sheaths would be expected to achieve different rates of fuel-air mixing. Each assembly was designed to permit changes in the gap height between the nozzle and the sheath. This variation would be expected to affect carbon deposition on the nozzle face.

Vaporizing Injectors

The two nozzles specified and supplied by NASA embodied the two more common fuel injection techniques--airblast and pressure atomization. UTRC felt that the third nozzle should be distinctly different from these devices in order to assess the potential of a new approach to achieve acceptable fuel introduction. A vaporizing concept was adopted. In a nozzle following this approach, the fuel would be injected onto the inner walls of a tubular device which is immersed in

the combustor primary zone. The hot wall temperatures would cause a portion of the fuel to vaporize and subsequently mix with the air flowing through the tube. A shroud of liner airflow would be used on the outside of the vaporizer to prevent excessive tube wall temperatures. Previous experience indicates that, in fact, the degree of vaporization achieved is low (less than 30 percent). Nevertheless, the vaporizer does offer the potential for sufficient fuel-air preparation to reduce soot formation. Additionally, it is an approach to achieve circumferentially distributed fuel injection, which should result in improved turbine inlet temperature pattern factors.

A successful vaporizer design would be one which effectively trades-off several conflicting characteristics. That is, while high surface area devices would be desirable to achieve a high degree of vaporization, they would also pose the greatest challenge to controlling metal temperatures to within acceptable limits. Additionally, while high design equivalence ratios within the vaporizer would minimize the likelihood for flashback in the tube, fuel decomposition/ cracking problems would be maximized. These characteristics must be carefully considered in designing a vaporizer.

Vaporizing injectors have been extensively investigated by the British aircraft industry and are employed in some commercial powerplants. Highly efficient, low smoke combustion has been attained. PWC has recently initiated an investigation of vaporizing injectors with the goal of developing a device suitable for the JT15D. Their experience guided the two vaporizer designs studied in this program. One vaporizer design, patterned after devices common to the British aviation industry, was the T-vaporizer (Fig. 8). Fuel was injected on the vaporizer walls in the stem region of the T and proceeded to partially vaporize and mix with the injector airflow prior to exiting from each end. The injected flow was directed toward the liner dome to enhance combustor stability and assure complete consumption of the fuel. The injector design equivalence ratio was approximately 3.6. The shroud airflow was variable to permit evaluation of differing vaporizer wall temperatures. The second vaporizer design, designated as a bar-vaporizer (Fig. 9) was based on PWC test experience. Test results indicated that a distributed source of fuel-air mixture enhanced the idle combustion efficiency and stability. Hence rows of holes were incorporated into the vaporizer design as indicated in the figure, with their orientation favoring the combustor dome. This device also had a design equivalence ratio of 3.6, and utilized a variable flowrate air shroud.

SECTION III - TEST FACILITY AND INSTRUMENTATION

The test program was conducted in the Jet Burner Test Stand (JBTS) located at UTRC. This section of the report describes the test facility, including the air and fuel delivery systems. Also specified are the test rig instrumentation including a description of the exit plane thermocouple and smoke probe arrays, the data acquisition system and data reduction procedures.

Test Facility

The test facility assembled for this program is shown schematically in Fig. 10. The facility consisted of an air inlet section, test section, and exhaust section.

The air inlet section provided airflow to the test section which satisfied the requirements of the test matrix. Air is supplied to the JBTS by multi-staged reciprocating compressors which can provide continuous airflow rates up to 2.0 kg/s at pressures up to 4.0 MPa. The flowrate to the rig was determined using an ASME venturi sized to operate choked. An electrical resistance-type air heater capable of heating airflows in excess of 1.5 kg/s to 600K was used; airflows up to 0.5 kg/s can be heated to 900K. The heated air was delivered to the plenum containing a 60-deg sector of a JT15D annular combustor. (The combustor model is described in detail in Section II of this report.).

The exhaust section contained two important components--a viewport and a back-pressure valve. The viewport was a 7.6-cm dia quartz window which provided direct observation of the combustor exit plane via an available closed-circuit color television system. The video image was monitored in the control room and recorded with an audio track to provide a permanent record of the test sequence. A remotely operated back pressure valve was used to control the test section pressure. A high pressure water quench was used to reduce the gas temperatures upstream of the valve to less than 700K to prevent damage to it.

Two test fuels were used in the program: Jet-A and a NASA-specified and supplied Experimental Referee Broad Specification fuel (ERBS). Jet A is the high quality fuel routinely used for commercial aviation. It has a relatively high hydrogen and low aromatic content, characteristics which tend to minimize smoke production. The specification for ERBS fuel has been established to reflect properties that might exist in future aviation fuels. ERBS has a lower hydrogen and higher aromatic content than Jet A (Table 1), which would favor smoke production. These chemical properties as well as the other properties contained in Table 1 indicate that ERBS has many similarities to No. 2 petroleum distillate fuel oil. The first two phases of the test program were performed using Jet-A fuel. This fuel was delivered to the combustor model from an

underground storage tank at the JBTS with a system capable of producing pressures up to 9.0 MPa. The ERBS fuel was used for a cycle test and was delivered to the combustor model via a batch (i.e., single drum) fuel system at pressures up to 6.8 MPa. The fuel systems were plumbed to feed a common manifold into the combustor model; high pressure gaseous nitrogen was available to purge the fuel from all sections of this manifold at the conclusion of a test.

Instrumentation

The test rig was instrumented according to standard practices; the instrumentation used is tabulated in Table 3. The test section airflow was determined using an ASME venturi located upstream of the main air heater; it was sized to operate choked for all test conditions. The volume flow of Jet-A fuel and ERBS fuel was determined with turbine meters calibrated with the appropriate fuel. Pressures and temperatures were measured by pressure transducers and thermocouples, respectively, selected to have the appropriate calibration ranges. Three total pressure measurements and two temperature measurements were made across the model inlet downstream of the perforated plate to determine the degree of flow uniformity. Pressure measurements were made on the combustor model to determine the pressure downstream of the baffle and within the combustor liner; differential pressure transducers were also employed to directly measure the pressure loss across the baffle and across the combustor liner. Three thermocouples were attached on the outside of the transition duct to determine its temperature level. The side wall coolant flow rate and temperature rise were also measured.

The flow exiting the combustor was documented using three steam-cooled smoke probes and 22 high temperature thermocouples (Fig. 11). The smoke probes, designed in accordance with SAE ARP1179, had an orifice sized to achieve isokinetic sampling of the exhaust stream at the cruise test condition. Two consecutive smoke samples were obtained from each smoke probe. The captured samples were transferred in electrically heated lines to a console which metered the flow rate and total volume flow of the sample. A smoke sample was acquired on Wattman No. 4 paper in accordance with the recommended practice and subsequently evaluated by the reflectance technique. Six water cooled struts supported the 22 radiation-shielded, Pt6Rh/Pt30Rh thermocouples. The material used for the exposed portion of the thermocouple sheath and the radiation shield was a platinum alloy providing a significant maximum temperature safety margin. (The thermocouple temperature limit of 1900K allowed a maximum exit temperature pattern factor of approximately 0.8).

Several key test parameters were monitored in the test cell control room during the experiment, including airflow venturi upstream pressure, heater exit temperature, combustor inlet temperature and pressure, combustor exit pressure and eight selected exit temperatures, baffle and liner pressure loss, fuel flow

rate, probe coolant temperature, and side wall coolant flowrate and temperature. The complete set of test data was recorded by means of an automatic data acquisition system which stored the information on magnetic tape for subsequent computer processing. The data system accepted data on up to 25 channels, 10 provided with signal conditioners, and the remainder compatible with the preconditioned inlet signals. The system was capable of controlling and accepting data from submultiplexers such as pressure and thermocouple scanning switches. The data channels were scanned sequentially at the rate of 12 channels per second and whenever a submultiplexer was connected to a channel, all ports or stations were sampled before proceeding to the next channel. An analog-to-digital converter digitized the data and an incremental magnetic tape recorder stored it for subsequent computer processing. The format of the tape was structured for compatibility with the UTRC UNIVAC 1110 digital computer.

The recorded data were used to compute several parameters which characterized the test condition and results including (symbol designated in the Instrumentation List, Table 3):

Airflow Rate, WA

The airflow rate was calculated from the equation for choked flow for a venturi. The venturi throat-to-upstream pressure ratio was calculated to verify that choked flow was attained.

WA = Function (PVUP,PVTH,TVUP)

Combustor Inlet Pressure, PT3

The inlet pressure was the calculated average of the three total pressure measurements located downstream of the inlet perforated plate.

PT3 = Average (PT31,PT32,PT33)

Combustor Inlet Temperature, TT3

The inlet temperature was the average of two temperature measurements located downstream of the inlet perforated plate.

TT3 = Average (TT31,TT32)

Combustor Exit Pressure, P4

The combustor exit pressure was the average of two wall pressure measurements located in the model exit transition duct.

P4 = Average (P41,P42)

Baffle Downstream Pressure, P3B

The pressure downstream of the baffle located in the liner airflow passage was the average of two pressure measurements.

P3B = Average (P3B1,P3B2)

Liner Pressure Loss, DPL/PT3

The fractional pressure loss across the liner was the quotient of the measured liner differential pressure and PT3.

Baffle Pressure Loss, DPB/PT3

The fractional pressure loss across the baffle was the quotient of the measured baffle differential pressure and PT3.

Combustor Reference Velocity, VREF

The combustor reference velocity was calculated using WA, PT3, TT3 and the maximum cross-sectional area within the combustor case.

Fuel Flow, WF

The fuel flow was calculated from the frequency output from a turbine meter calibrated with the test fuel, accounting for density changes by measuring the fuel temperature.

WF = Function (WF,TFINJ)

For the spill return injector, both the delivered and returned flowrates were metered, and a net fuel flow to the combustor calculated.

Fuel-Air Ratio, FA

The fuel-air ratio was the quotient of the metered flowrates.

FA = WF/WA

Primary Zone Equivalence Ratio, ϕP

The equivalence ratio in the primary zone was based on the airflow entering the primary zone and the fuel flow. The primary airflow depended on the total

airflow, the pressure loss across the baffle, and the test configurations (i.e., all nozzle/swirler/shroud configurations did not have the same effective airflow area).

$$\Phi P = \text{Function (WA,WF,DPBAF,configuration)}$$

Ideal Exit Temperature, T4IDL

The ideal combustor exit temperature was calculated using a standard thermochemical calculation procedure.

$$\text{T4IDL} = \text{Function (PT3,TT3,F/A,fuel properties)}$$

Combustor Exit Temperature, T4

The combustor exit temperature was the average of 22 temperature measurements.

$$\text{T4} = \text{Average (T41,T42, . . . T422)}$$

Combustor Efficiency, ETAT

The combustor efficiency was the quotient of actual-to-ideal temperature rise across the combustor.

$$\text{ETAT} = (\text{T4}-\text{TT3})/(\text{T4IDL}-\text{TT3})$$

Pattern Factor, PF

The pattern factor was the greatest exit temperature deviation from the average value, normalized by the combustor temperature rise.

$$\text{PF} = (\text{T4i}-\text{T4})_{max}/(\text{T4}-\text{TT3})$$

where T4i denotes any individual exit temperature measurement.

Smoke Number, SN

The smoke number was calculated from the reflectance of the clean filter paper (RC) and of the sample filter paper (RS).

$$\text{SN} = 100\ (1 - \frac{\text{RS}}{\text{RC}})$$

SECTION IV - TEST PROGRAM

This section of the report presents (1) the Test Plan and (2) the results of the experimental investigation. The test program proceeded in three phases, with each successive phase attempting to narrow the initial list of fuel injection candidates. The order of presentation of the test results will follow this phase plan.

Test Plan

The purpose of the tests was to document soot formation (exhaust smoke) and carbon deposition using several configurations of fuel nozzle/swirler/shroud. It was important to recognize that the testing must be intermittent. That is, while smoke generation could be determined by an on-line technique, it was necessary to terminate the test to observe and record the carbon deposition. Therefore, the test periods for any condition were limited to 30 minutes and always followed by a visual inspection of the combustor interior. Recognizing that such intermittent testing would be time consuming, it was necessary to construct a test plan which would permit identification of the most promising nozzle/swirler/shroud configurations and focus on them for more in-depth characterization. Therefore, the testing was conducted in three phases: configuration screening, envelope definition and cycle performance.

Phase I - Configuration Screening

Combinations of swirlers and shrouds were investigated for each of four fuel nozzles--splash cone injector, a spill return injector, and two vaporizer injectors. A total of 16 combinations of test hardware were available for investigation. However, because of the test period limitations, only ten of these combinations were studied. The selected configurations were tested at the idle and SLTO test conditions specified in Table 4. The results from these configuration screening tests were used to select the two most promising concepts. Particular importance was given to evaluating the smoke emissions, carbon formation, combustor exit temperature pattern factor, and combustion efficiency at each test condition.

Phase II - Envelope Definition

The screening tests conducted in Phase I identified two hardware configurations which minimize the formation of carbonaceous species at selected standard operating conditions. The Phase II tests parametrically investigated the influence of four variables on soot formation and carbon deposition for these configurations in an attempt to define parameter threshold values for acceptable operation. Similar to the Sceening Tests, the parametric tests also required that the rig be inspected for carbon deposition; hence the envelope definition tests were intermittent.

The parametric tests were conducted by first establishing a baseline condition, chosen to be the cruise condition shown in Table 4, and subsequently performing tests at two additional values for each parameter. The four parameters investigated included combustor pressure, primary zone equivalence ratio, combustor loading and combustor inlet temperature.

Phase III - Cycle Performance

It was recognized that carbon deposits which form at one condition may be affected by transition to and operation at a subsequent condition. Therefore, a cycle test was performed to simulate the deposits that would accumulate in a burner after several missions. This test was performed with Jet-A fuel and with ERBS fuel to document the effect of a broadened specification fuel. The cycle was an adaptation of the EPA landing/takeoff cycle, and included specified time periods at idle, sea-level-takeoff and cruise conditions as follows: idle--19 min, SLTO--3 min, cruise--15 min. The test consisted of three repetitions of the cycle and concluded with an additional 15 minutes of idle operation.

Test Results

Phase I - Configuration Screening

The characteristics of nozzle/swirler/shroud configurations for each of the four injectors tested were adequately revealed in the screening investigations. That is, devices with desirable characteristics and those with ineffective or underdeveloped characteristics were readily identified.

Tests with configurations embodying the splash cone injector indicated it to be an ineffective nozzle. As indicated in Section II, the nozzles received from NASA appeared to be not of sufficiently high quality to operate in a repeatable fashion. Combustor exit temperature patterns obtained in the first test indicated that the two nozzles were not well matched. Subsequent inspection revealed that not all orifices on each nozzle were open, a condition identical to that observed in the initial ambient fuel spray tests. Attempts to remedy this problem were unsuccessful. That is, despite the use of fine wires and solvents to open the orifices, acceptable nozzle performance was not attained. Hence, no specific test results are reported for the splash cone nozzle.

The spill return was a high quality injector which produced a uniform hollow-cone fuel spray. Tests were performed with this nozzle with both nozzle sheaths depicted in Fig. 7, and with nozzle face-to-sheath gap heights of 0.50 mm and 0.25 mm for each. In general, these configurations achieved highly efficient combustion with minimal carbon deposition. No carbon deposits were observed after tests at the SLTO condition. A soft carbon deposit was formed on the nozzle and sheath faces for tests at the idle condition; no carbon deposits were observed on any portion of the liner. This carbon layer was formed using either sheath (Fig. 12) and for both gap heights.

The combustor exit characteristics of the four spill return configurations are compared in Table 5. The swirler sheath was apparently more effective in mixing the fuel and air near the nozzle, resulting in significantly lower average smoke numbers (SN) than achieved with the non-swirl sheath. While the attractive mixing characteristics of swirling flows is generally acknowledged, the superior performance of the swirler device was unexpected because the JT15D, a low smoke engine, employs the non-swirl device. Perhaps this result indicates that, in many instances, hardware components are combustor-specific, emphasizing that results from test rigs which mix components from different combustors indicate trends only. The mixing characteristics of the swirler sheath were also evidenced by generally smaller variations in the smoke numbers and lower temperature pattern factors (PF). The smoke number variation was substantial for all cases however. The maximum SN was attained from the sample extracted midway between nozzles, indicating the presence of locally fuel-rich regions because of fuel spray overlap. Use of the smaller gap height promoted lower smoke numbers with both sheaths. Apparently, the airflow passed by the larger gap, in an attempt to cleanse the nozzle face, altered the airflow pattern enough to degrade the fuel-air mixing process adjacent to the nozzle. Furthermore, this increased airflow was no more effective at preventing carbon deposition on the nozzle face.

Test results obtained with the bar-vaporizer configuration were quite conclusive; it experienced significant damage in the first test at the SLTO condition (Fig. 13). The design used evolved from PWC experience at simulated idle test conditions. In the more hostile environment at SLTO, the ends of the bar burned, indicating insufficient cooling. The bar-vaporizer design ejected a fuel-air mixture along the bar in an attempt to attain a distributed fuel injection. Apparently insufficient flow remained at the ends of the bar, resulting in the observed destruction. The hole diameters increased along the bar, being 4.6 mm near the stem and 5.6 mm near the end cap. Possibly a steeper graduation would result in adequate air flow at the end of the bar to assure vaporizer survival.

Tests with the T-vaporizer were performed at the idle and SLTO test conditions for a shroud airflow equal to approximately 3 percent of the combustor airflow and for zero shroud airflow. The results for these T-vaporizer configurations are indicated in Table 6. Average smoke numbers considerably lower than observed with the spill return nozzle were attained, especially at the idle condition; a smaller variation in SN was also evident.

The pattern factor was comparable to the spill return values for the 3 percent shroud airflow configuration, but unacceptably high for zero shroud airflow. It would be expected that the higher vaporizer wall temperatures associated with zero shroud air-flow would increase the rate of fuel vaporization, permitting greater fuel-air mixing within the injector. While such an occurrence

would generally be expected to result in more uniform combustor temperatures, the opposite trend was observed. Perhaps this indicated a need to achieve more vigorous mixing within the combustor. That is, the equivalence ratio of the vaporized fuel-air mixtures could exceed unity, resulting in locally hot regions at the combustor exit if adequate streamtube mixing did not occur.

A film of soft carbon was deposited on a portion of the T-vaporizer external surface. The film was present after tests at both idle and SLTO conditions and for both levels of shroud airflow. Figure 14 depicts a typical carbon deposit pattern. The layer is heaviest on the stem and covers the central region of the crossbar. The pattern shown developed in tests with 3 percent shroud airflow. The level of deposition diminished for zero shroud airflow, being confined to the vaporizer stem only. Apparently the higher metal temperatures were unfavorable to the deposition processes. It is noted that no other carbon deposition was observed. Carbon deposits were not observed on any portion of the liner, nor was there any evidence of fuel coking within the vaporizer.

Inspection of the two T-vaporizers after tests at the SLTO condition revealed that one end of one vaporizer was significantly burned (Fig. 13). It was peculiar that only one vaporizer experienced this failure, and that the end affected was not in the region between the injectors but toward a combustor model sidewall. The vaporizer was repaired once but subsequently failed in a similar manner. The vaporizers exhibited no distress after tests at the idle condition.

The cause of the one vaporizer failure pattern is not known. During Phase II, tests were performed at the cruise condition with another (but geometrically identical) combustor liner, and with an unrepaired vaporizer. No additional distress was experienced despite operation with a primary zone which was as hostile as the one associated with the SLTO condition. Hence it is suspected that the failure was linked with use of the original combustor liner. No other data are available to substantiate or refute this thesis.

Phase II - Envelope Definition

Based upon the injector configuration characteristics observed during the Phase I testing, one spill return and one T-vaporizer configuration were chosen for additional investigation. The spill return configuration utilized the swirler sheath positioned to give a nozzle face-to-sheath gap height of 0.25 mm. The vaporizer configuration was set to deliver a 2 percent shroud airflow. This level was less than investigated in Phase I in an attempt to reduce the carbon deposition on the vaporizer surfaces.

Envelope definition tests investigated the influence of combustor inlet air temperature, combustor pressure, primary zone equivalence ratio and combustor loading on the characteristics of the chosen configurations. Because of constraints on the test program, the investigation of the T-vaporizer was limited to assessing the inlet air temperature influence. A summary of the changes in combustor characteristics observed during the envelope definition tests is presented in Table 7.

Variations of inlet air temperature would be expected to affect both the soot formation and carbon deposition processes. The tests performed were based on the cruise test condition, with parametric variation of the inlet air temperature down to 300K. Figure 16 displays the observed influence on soot formation as represented by the average combustor exit smoke number. For both nozzle configurations, the smoke values increased rapidly with reduced air temperature. The particular susceptability of the vaporizer to this influence was evidenced by a steeper slope of this trend. In these tests the combustor exit temperature pattern factor indicated regions of progressively higher fuel concentration. That is, the decrease in inlet temperature from 590K to 300K raised the spill return configuration PF from 0.31 to 0.38 while the vaporizer configuration PF rose from 0.29 to 0.47. Thus the change in inlet air temperature affected the gross mixing patterns in the burner through changes in the combustor reference velocity. Regions of higher fuel concentration resulted which were favorable to soot production. In addition the decrease in final combustion gas temperature would oxidize less of the soot formed, leading to significant increases in the exhaust smoke. There was no significant change in the level of carbon deposited on the spill return nozzle for the investigated range of inlet temperature. This temperature change however resulted in a substantial carbonaceous growth from one of the vaporizers (Fig. 17), with smaller carbonaceous solids on the other device. Clearly, prolonged operation of this vaporizer at very low inlet air temperatures (as might be experienced at idle on an artic day) would not be acceptable.

Investigations of the influence of combustor pressure were performed by varying the position of the test rig back-pressure valve while holding airflow, fuel flow and inlet temperature constant. Therefore while the combustor loading and overall fuel-air ratios were held constant, the reference velocity diminished as the combustor pressure was elevated. Increased combustor pressures promoted smoke formation by the spill return configuration (Fig. 18) while the combustor pattern factor was not affected. This latter observation indicated that fuel distribution gross combustor mixing patterns were minimally affected. Hence, the results indicated that the chemical mechanisms responsible for soot formation were accelerated.

Increases in the primary zone equivalence ratio would be expected to favor soot formation because of increased fuel concentrations. Tests were performed to investigate this influence by actuating the baffle to an extreme position.

In such a position, the primary airflow was reduced from 27 percent to 24 percent of the total combustor airflow; simultaneously, the primary zone equivalence ratio increased from 1.0 to 1.16. This range was insufficient to promote a significant increase in average smoke number (the observed change was SN=10 to SN=13). The temperature pattern factor increased significantly, however, from PF=0.30 to PF=0.38 reflecting an alteration of the airflow patterns within the combustor. While an increase in PF would be expected to indicate degraded mixing processes, the similar values of average smoke number (and SN variation) indicated comparable mixing rates. These observations were not necessarily in conflict as the combustor exit PF was likely governed by the combustor gross mixing rates while the soot production was controlled by mixing rates near the injector.

Tests were performed to assess the influence of higher combustor loading. The inlet temperature, combustor pressure and overall fuel-air ratio were held constant while increasing the magnitude of both the fuel and airflow. As a result, combustor reference velocity also increased with combustor loading. The reference condition again was the cruise test condition, with loadings up to 175 pct of cruise loading investigated.

Very low smoke levels were attained under increased combustor loading conditions, with average smoke numbers less than five. This was attributed both to higher mixing rates which accompany increased reference velocity and to an improved fuel atomization with increased fuel flow. The increase in reference velocity resulted in a corresponding increase in the airflow jet velocity through the liner and nozzle sheath, promoting the fuel-air mixing near the nozzle required to prevent soot formation. Improved atomization further suppressed any tendency to form locally fuel-rich regions favorable to soot production.

The increased loading did result in one undesirable characteristic--the combustion efficiency decreased significantly with increased loading (Fig. 19). Since mixing rates appeared adequate to produce low smoke and pattern factors comparable to the cruise condition, the lower efficiency was attributed to insufficient combustor residence time. At the cruise condition, the residence time (based on the exit gas temperature) was approximately 8 ms, reducing to approximately 4 ms at the highest loading investigated. Such a change can significantly reduce the levels of both fuel vaporization and oxidation. That is, lower degrees of fuel vaporization could be experienced because of less residence time in the primary zone, forcing the final oxidation steps, particularly CO oxidation, further into the dilution zone. In this area, the lower gas temperatures would retard the CO oxidation rate, allowing products of incomplete combustion to exit the burner. This problem could be lessened by achieving finer fuel atomization.

Phase III - Cycle Performance

Cycle tests were performed with the spill return injector configuration using both Jet A and ERBS fuel. The tests consisted of three repetitions of the 37 minute idle/SLTO/cruise cycle described earlier, and concluded with additional idle operation for a total test duration of 126 minutes.

The intended purpose of these tests was to permit the accummulation of carbon deposits over a longer test period as they would be influenced by a changing operating condition similar to that experienced in an operational engine. As indicated in discussions of the Phase I and II test results, the carbon deposits at any single condition were minimal for the spill return configuration. Hence it was not surprising to find minimal carbon deposits after the cycle tests. This observation was true for tests with either Jet A or ERBS fuel. Only a light film of soft carbon was discovered on the nozzle and swirler sheath faces; no carbon deposits were found on any portion of the combustor liner.

Smoke samples were extracted during the cycle test during operation at the idle and cruise test conditions; the opeating period at the SLTO condition was too brief to acquire smoke samples. The average smoke numbers, at both idle and cruise test conditions, were greater when operating on ERBS fuel than on Jet A. The values nearly doubled at both conditions, going from SN=30 to SN=53 at idle, and SN=10 to SN=19 at cruise. Such increases were similar to those reported by other investigators (Refs. 3, 4, 5) who correlated experimental combustor smoke emissions with fuel hydrogen content. Hence if lower hydrogen content fuels gain common usage as aviation fuels, improvements to the fuel atomization, fuel-air mixing near the injector and/or primary zone stoichiometry will be required to retain acceptable exhaust smoke levels.

Comparison with NASA Studies

Two of the nozzles investigated in this program were specified by NASA--namely, the splash-cone and spill return injectors. These devices were selected because of capabilities demonstrated in previous NASA studies (Ref. 2 and 6) of a model gas turbine combustor. The NASA study utilized a fully-annular, reverse flow combustor with a liner outer diameter of 38.5 cm, and an annulus height of 5 cm. The liner was configured to accept either 6, 9, 12 or 18 equally-spaced fuel injectors. The majority of tests performed utilized the eighteen nozzle array, which corresponded to a nozzle density approximately 50 percent higher than the JT15D array used in the UTRC program. Tests were performed over a range of conditions up to SLTO corresponding to a 16:1 compression ratio engine. Average exhaust emissions, gaseous and particulate, and temperature distribution were determined.

Seven nozzles were studied to investigate pressure-atomizing, air-blast, impingement and air-assist fuel injection techniques. The splash cone and spill return nozzles were the best performing of these injectors. The splash cone injectors promoted complete combustion at high power conditions but were unable to sustain any combustion at idle. Use of a fuel sectoring technique permitted highly efficient, low power operation. Low exhaust emissions were achieved; the average smoke number was 15 at SLTO, reducing to less than 5 at lower power conditions. A temperature pattern factor of 0.2 was attained at high power conditions. These characteristics would make the splash-cone injector an attractive nozzle for a small gas turbine combustor application, and justify further study of it. Obviously, however, the quality of the devices tested by NASA was superior to the splash cone injectors supplied to UTRC. As discussed earlier, no comparative data were obtained.

The spill return nozzles also achieved desirable performance characteristics. A 100-percent combustion efficiency was achieved at high power conditions, decreasing only to 92 percent at idle. This relatively high performance was sustained because of the spill flow feature. That is, it was able to use high spin chamber velocities to sustain high levels of atomization even for idle operation. High efficiencies were also observed in the UTRC program. Precise efficiencies were not determined at idle--the exit temperature was extremely non-uniform causing errors in the temperature rise efficiency because of non-representative flow. However, a stable operation was attained with efficiencies believed to be higher than 90 percent. At high power, temperature pattern factor of approximately 0.26 was attained in the NASA study using an eighteen injector array, increasing the PF = 0.9 for a nine injector array. The UTRC configuration, representing a twelve injector array, achieved a PF = 0.3 indicating that more effective combustor mixing was attained. That is, a reasonable PF was achieved for an injector array 50 percent coarser than used by NASA. This observation was consistent with the expected higher turbulence levels in the JT15D, 2-percent pressure-loss liner, was contrasted with the NASA 1.5-percent pressure-loss device. Very low smoke numbers were attained at SLTO by NASA (SN less than 5), less than the SN = 22 values observed at UTRC. The NASA combustor emissions rose to approximately SN = 35 for tests performed with the SLTO airflow but with the fuel-air ratio reduced from 0.024 to 0.014. These data indicated a strong influence of combustor exit temperature on the exhaust smoke. That is, for the NASA SLTO tests at f/a = 0.024, an exit temperature of approximately 1500K would be achieved, reducing to approximately 1250K for f/a = 0.014. Higher soot oxidation rates would be achieved at the higher temperatures, resulting in the very low SN. The UTRC SLTO condition produced an exit temperature of approximately 1300K; the observed SN = 22 level was consistent with the response of soot oxidation to exit temperature. A near doubling of smoke levels for tests with ERBS fuel, compared to tests with Jet A fuel, was observed in both investigations of the spill return injector.

SECTION V - SUMMARY OF RESULTS

An evaluation of the ability of several fuel injection configurations to minimize carbon and soot formation in small gas turbine combustors without compromising other desirable performance characteristics has been performed. The major findings of this study can be summarized as follows:

1. No significant carbon deposits were formed during tests at standard engine operating conditions. This was true for both the spill return and vaporizing injector, whether using Jet A or ERBS Fuel. No deposits were observed on the combustor liner, soft carbon deposits were observed on the injector surfaces.

2. A large growth of carbonaceous material was observed on the vaporizing injector after tests performed with combustor inlet air at 300 K.

3. The lowest smoke emissions were achieved using a T-vaporizer injector. In contrast to the spill return injector, smoke numbers achieved at idle conditions with the vaporizer were very low (SN < 5).

4. Smoke produced by the spill return nozzle rates was dependent on the mixing near the nozzle. Swirling the nozzle-shroud airflow reduced the smoke production; excessive nozzle-face airflow increased the smoke production.

5. Tests with ERBS fuel resulted in smoke levels approximately twice the levels achieved with Jet A.

6. Reduced smoke emissions were achieved by operating the spill return injectors at high fuel flowrates to achieve a more highly atomized fuel spray.

7. Improved vaporizer design guidelines are required to produce more durable nozzles. Insufficient airflow at the ends of the bar-vaporizer resulted in burning of the ends of this injector. Adequate airflow along the length of a vaporizer must be provided in order to minimize fuel-rich conditions near the metal walls.

SECTION VI - CONCLUSIONS

A limited investigation of carbon and smoke formation in small gas turbine combustors has been conducted. Based upon observations in this program, the following conclusions can be formulated:

1. The ability of a combustor to achieve and sustain low smoke emission operation depends on the combustor fluid mechanics, the fuel spray atomization (and how these two features respond to changing combustor operation) and the fuel chemical properties. In particular, the likelihood of low smoke operation is enhanced by high rates of fuel-air mixing near the injector, fine atomization and high fuel hydrogen content.

2. Low carbon deposit operation can be attained for pressure-atomizing injectors.

3. Vaporizing fuel injectors can achieve very low smoke operation at all conditions. Current vaporizer design methodology is inadequate, however.

REFERENCES

1. Demetri, E. P., et al.: Study of Research and Development Requirements of Small Gas Turbine Combustors. NASA CR-159796, 1980.

2. Norgren, Carl T. and Stephen M. Riddlebaugh: Effect of Fuel Injector Type on Performance and Emissions on Reverse Flow Combustor. NASA TP1945, December 1981.

3. Butze, H. F. and R. C. Ehlers: Effect of Fuel Properties on Performance of a Single Aircraft Turojet Combustor. NASA TMX71789, October 1975.

4. Moses, C. A. and D. W. Naegeli: Combustor Performance of High Availability Fuels. Central States Section, Combustion Institute, 1978 Spring Technical Meeting, April 1978.

5. Blazowski, W. S. and T. A. Jackson: Evaluation of Future Jet Fuel Combustion Characteristics. AFAPL-TR-7793, July 1978.

6. Norgren, Carl T. and Stephen M. Riddlebaugh: Small Gas-Turbine Combustor Study -- Fuel Injector Evaluation. NASA TM 82641, July 1981.

TABLE 1

Typical JT15D-4 Operating Conditions

	Gnd Idle	SLTO	Cruise*
Net thrust (kN)	--	11	4
Engine airflow (kg/s)	2.4	9.5	5.3
Engine fuel flow (kg/hr)	87	618	342
Combustor inlet pressure (MPa)	0.18	1.02	0.56
Combustor inlet temperature (K)	375	635	593
Combustor pressure drop (pct)	2.21	2.03	1.95
Combustor fuel-air ratio (-)	0.010	0.0188	0.0188
Combustor exit temperature (K)	785	1291	1256

*Altitude condition at 7.6 km and flight Mach number = 0.6.

TABLE 2

Typical Fuel Properties

	Jet A	ERBS	No. 2
Specific gravity	0.81	0.84	0.85
Hydrogen content (wt pct)	13.7	12.9	12.8
Aromatic content (vol pct)	16	32	35
Heating value (J/g)	43000	41900	42000
Distillation temperature range (K)	440-540	440-620	440-600

TABLE 3

Instrumentation

(Note: PARAM1,2 denotes multiple measurements)

Parameter	Range	Description
Air Supply		
PVUP	4.0 MPa	Pressure upstream of airflow venturi
PVTH	3.0 MPa	Pressure at throat of airflow venturi
TVUP	Type K	Temperature upstream of airflow venturi
PHIN	3.0 MPa	Pressure at inlet to air heater
PHEX	250 psi	Pressure at exit of air heater
THEX	Type K	Temperature at exit of air heater
PPLEN	2.0 MPa	Pressure in plenum
TPLEN1,2	Type K	Temperature in plenum
Fuel Supply		
WF	4.0 LPM	Flowrate of fuel to model
WFRTN	1.0 LPM	Flowrate of return fuel
PFINJ	9.0 MPa	Pressure of fuel at rig
TFINJ	Type K	Temperature of fuel at rig
TFRTN	Type K	Temperature of return fuel
Model		
PT31,2,3	2.0 MPa	Pressure downstream of perforated plate
TT31,2	Type K	Temperature downstream of perforated plate
P3B1,2	2.0 MPa	Pressure downstream of baffle
P41,2	2.0 MPa	Pressure inside combustor liner
DPLINER	70 KPa	Differential pressure across liner
DPBAF	70 KPa	Differential pressure across baffle
TWSL	Type K	Temperature of left side wall
TWSR	Type K	Temperature of right side wall
TTDB1,2,3	Type K	Temperature on bottom of transition duct
TCSW	Type K	Temperature of side wall coolant
T4-1, . . . 22	Type B	Temperature at combustor exit
TCSP	Type K	Temperature of smoke probe coolant
TSAM1,2,3	Type K	Temperature of smoke sample exiting probe
TCTR	Type K	Temperature of transition spool coolant

TABLE 4

Test Conditions

	Idle	SLTO	Cruise
PT3 (MPa)	0.18	1.02	0.56
TT3 (K)	380	640	590
WA (kg/s)	0.4	1.5	0.8
VREF (m/s)	8	10	10
WF (kg/hr)	14.5	102	57
f/a	0.01	0.019	0.019
ϕ_P	0.5	1.0	1.0

TABLE 5

Spill Return Configuration Screening

Configuration	Sheath	Gap (mm)	Condition	SN_{ave}	$SN_{max}-SN_{min}$	PF
1	Non-swirl	0.50	IDLE	47	7	--
			SLTO	20	29	0.36
2		0.25	IDLE	33	20	--
			SLTO	25	26	0.45
3	Swirl	0.50	IDLE	19	19	--
			SLTO	29	40	0.36
4		0.25	IDLE	24	8	--
			SLTO	22	16	0.30

TABLE 6

T-Vaporizer Configuration Screening

Configuration	Shroud Airflow (pct)	Condition	SN_{ave}	$SN_{max}-SN_{min}$	PF
1	3	IDLE	3	6	--
		SLTO	12	12	0.34
2	0	IDLE	9	12	--
		SLTO	17	6	0.57

TABLE 7

Envelope Definition Test Results Summary

Configuration	Parameter Investigated	SN	PF	η_c pct
Spill return	Cruise - baseline	10	0.30	100
	T3 = 420K	16	0.30	100
	T3 = 300K	33	0.38	100
	P3 = 0.9 MPa	13	0.31	100
	P3 = 1.2 MPa	19	0.30	100
	ϕP = 1.15	13	0.37	100
	Loading = 140 pct	5	0.34	88
	Loading = 175 pct	2	0.34	83
T-Vaporizer	Cruise - baseline	7	0.29	100
	T3 = 420K	31	0.44	100
	T3 = 300K	62	0.47	100

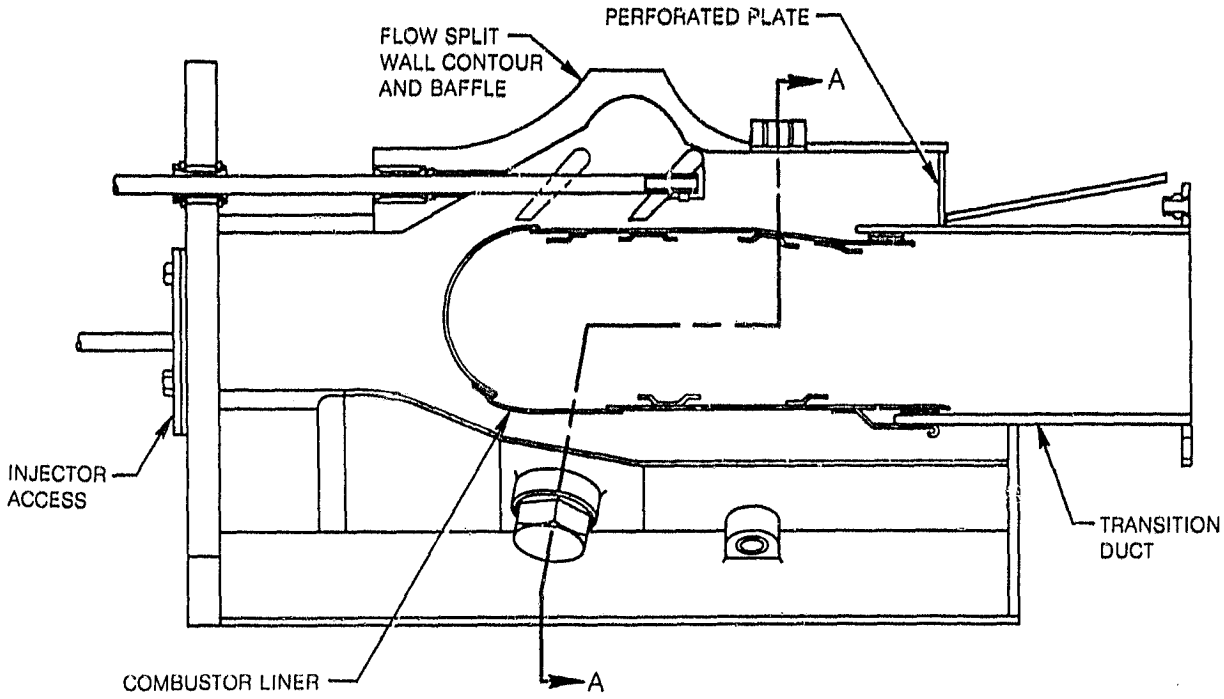

a) SIDE VIEW

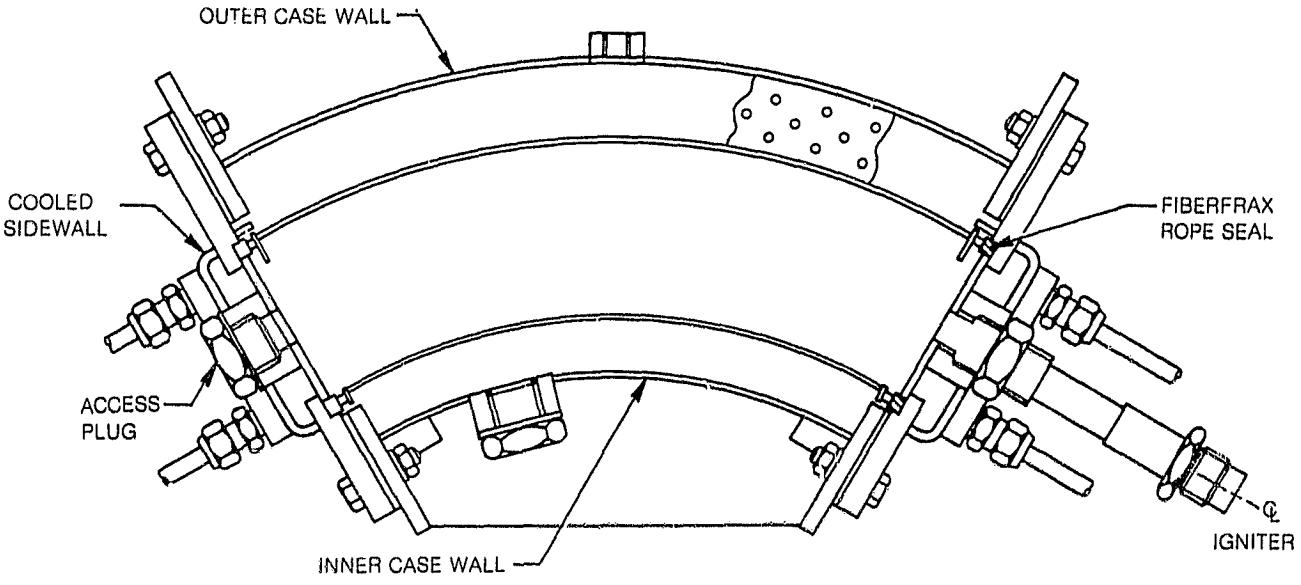

b) END VIEW (FULL SECTION ON A-A)

Fig. 1 Sectional View of JT15D Combustor Model

81–1–36–1

a) VIEW FROM EXIT

b) VIEW FROM DOME

Fig. 2 JT15D Model Combustor Assembly

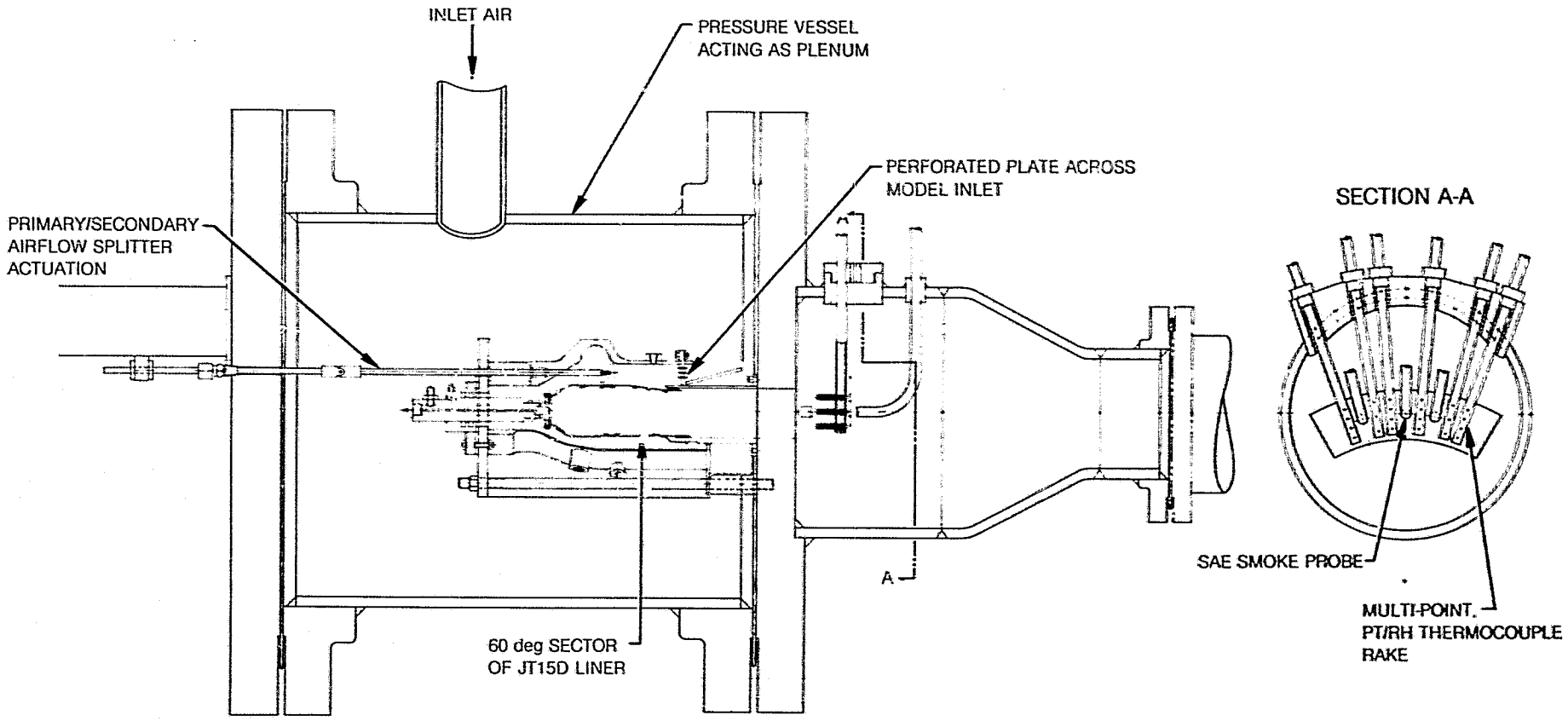

Fig. 3 Model Combustor Containment

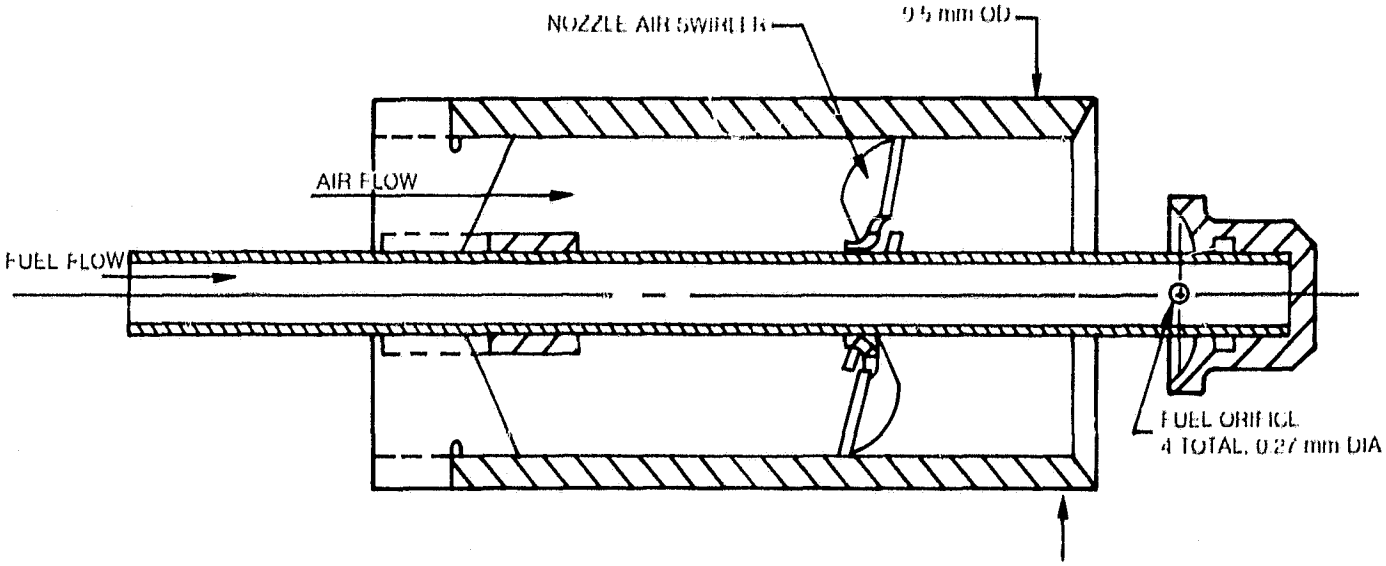

Fig. 4 Splash Cone Injector

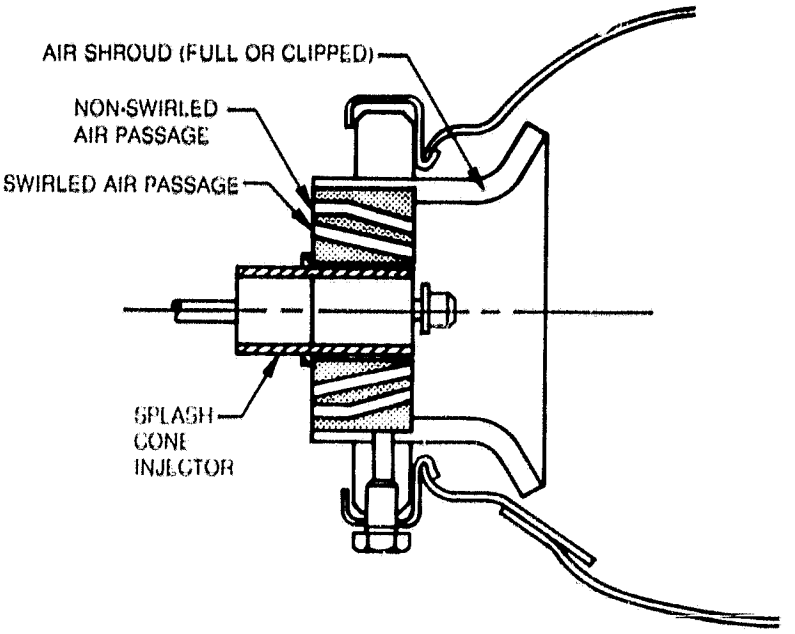

a) PARTIAL SWIRL CONFIGURATION

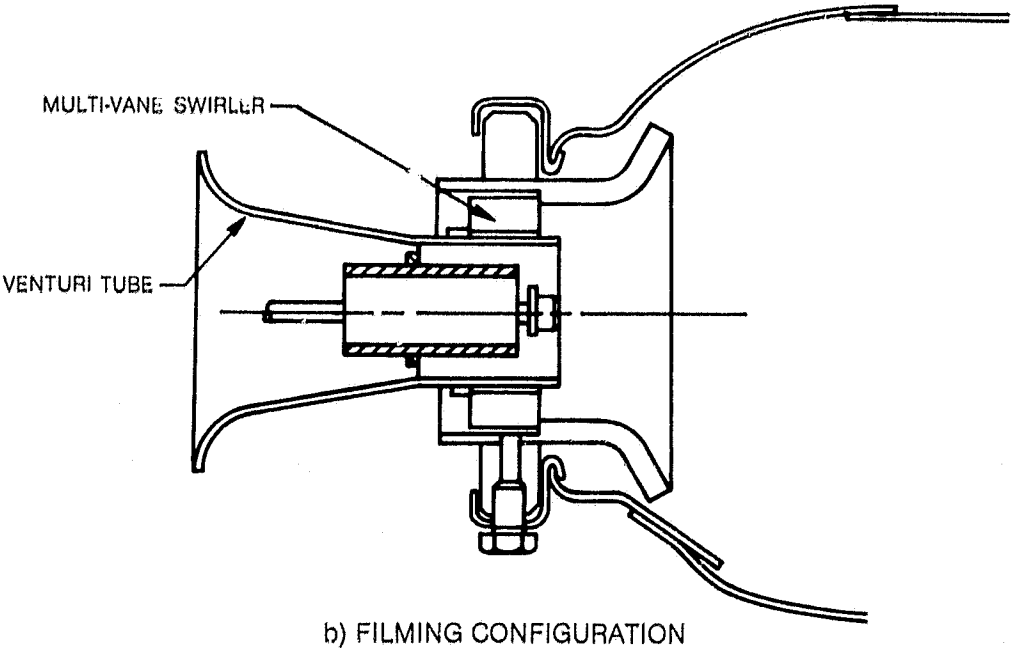

b) FILMING CONFIGURATION

Fig. 5 Air Shroud-Swirler Assemblies for Splash Cone Injector

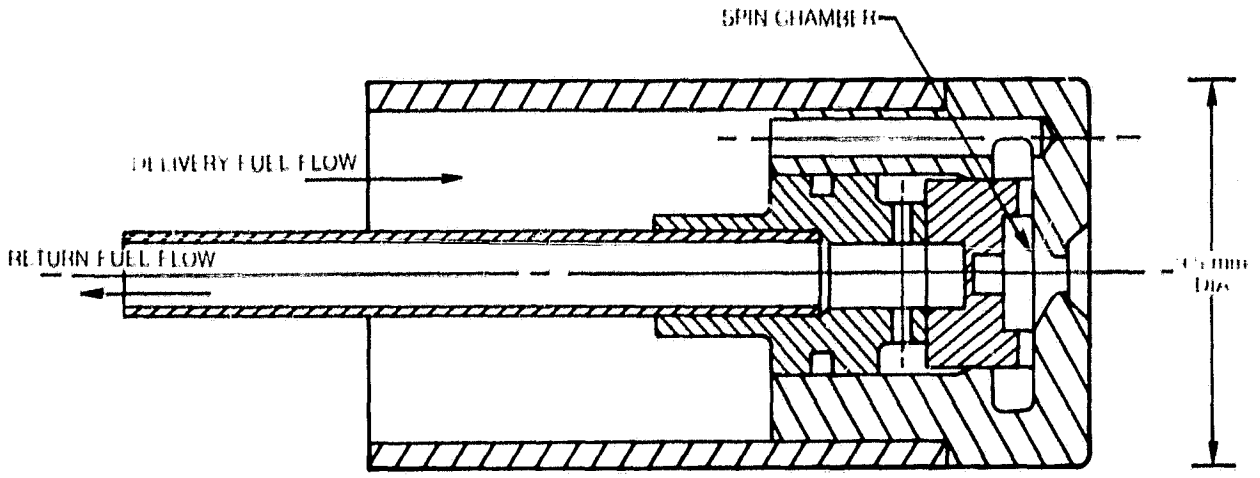

Fig. 6 Spill Return Injector

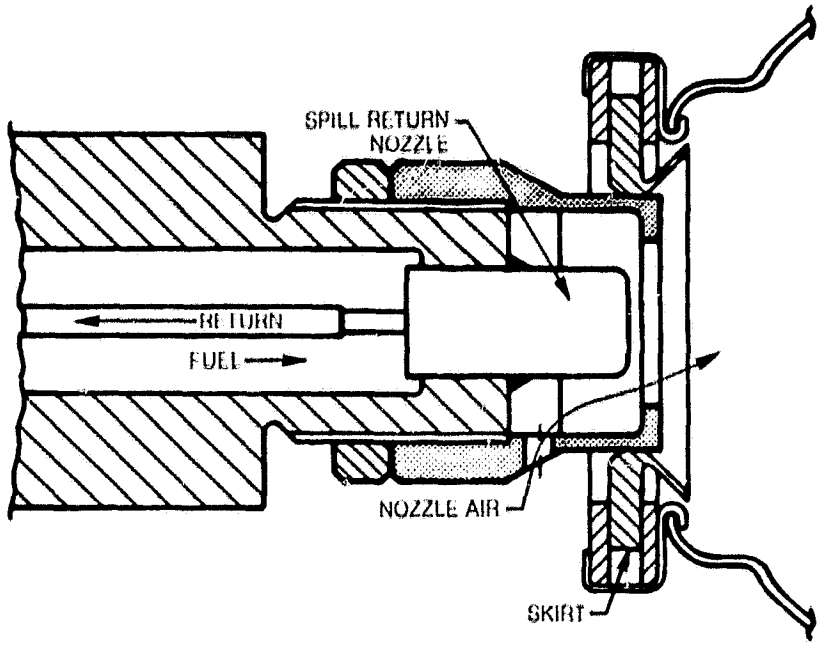

a. NON-SWIRL SHEATH

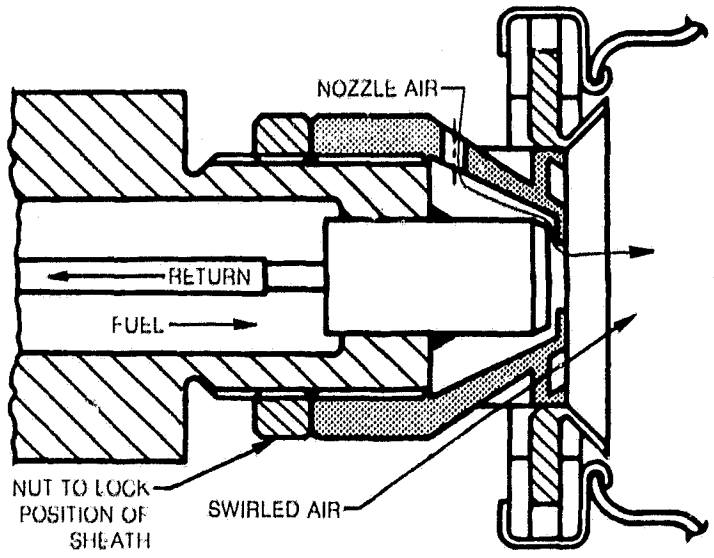

b. SWIRLER SHEATH

Fig. 7 Air Shroud-Swirler Assemblies for Spill Return Injector

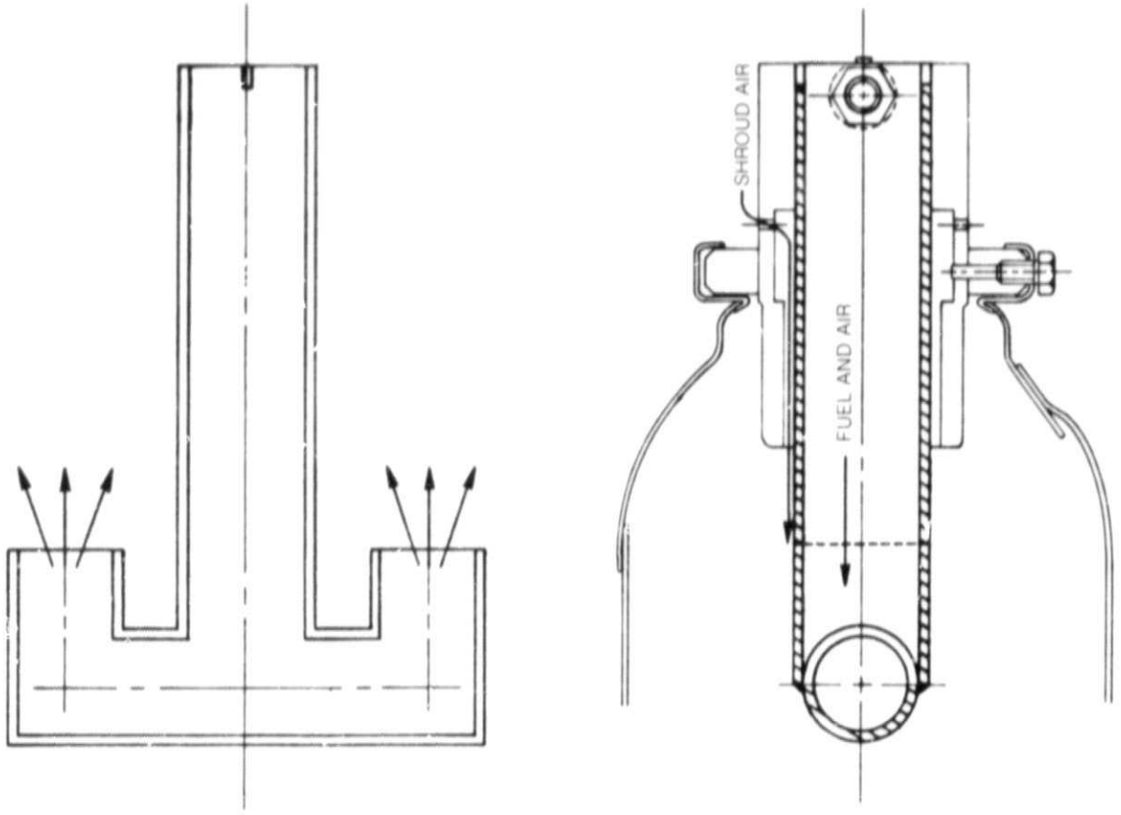

Fig. 8 T-Vaporizer Assembly

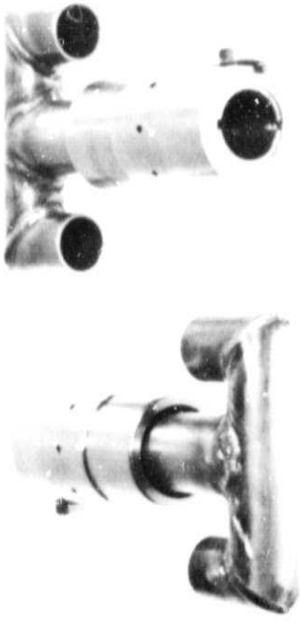

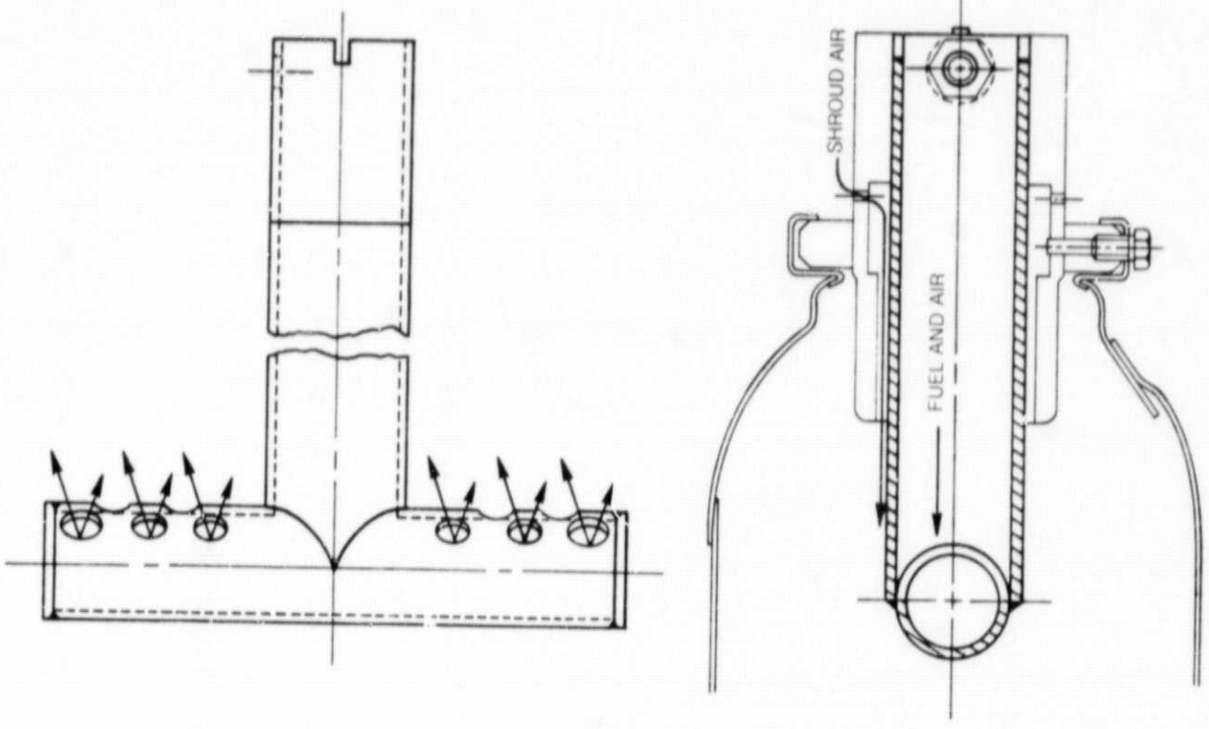

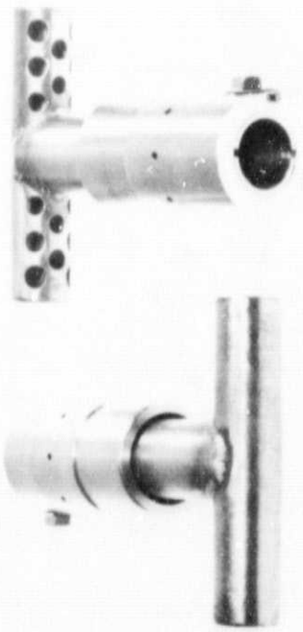

Fig. 9 Bar Vaporizer Assembly

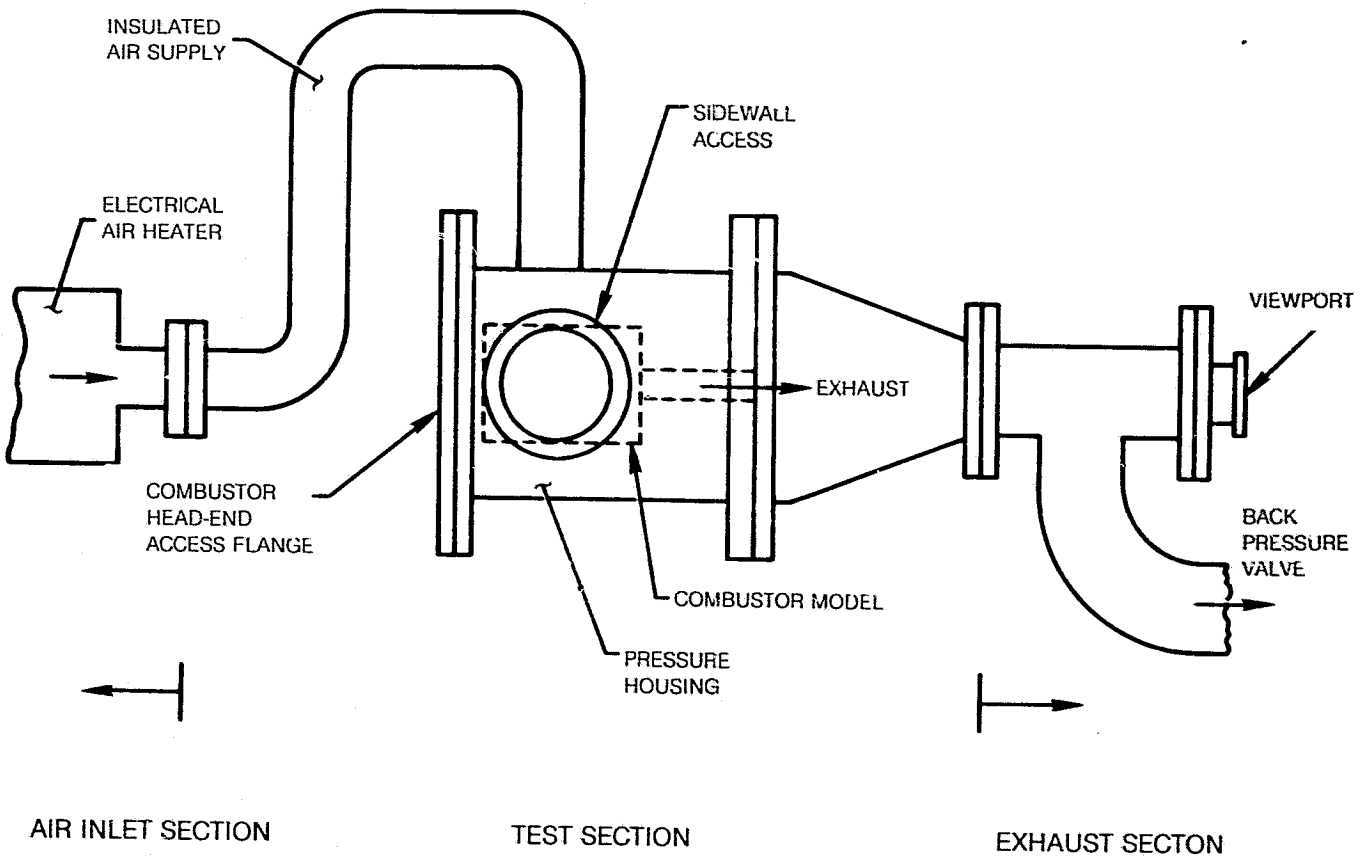

Fig. 10 JT15D Combustor Test Facility

a) INSTRUMENTATION LAYOUT

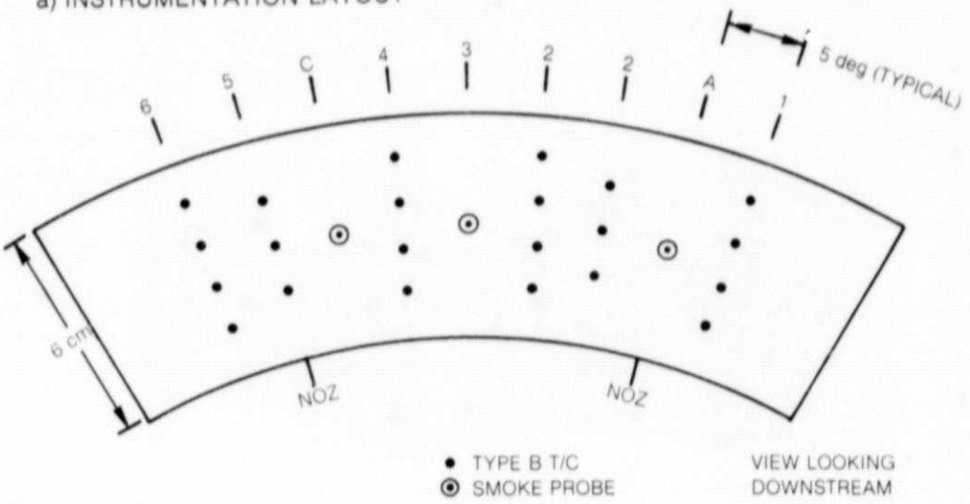

b) DIAGNOSTIC PROBES

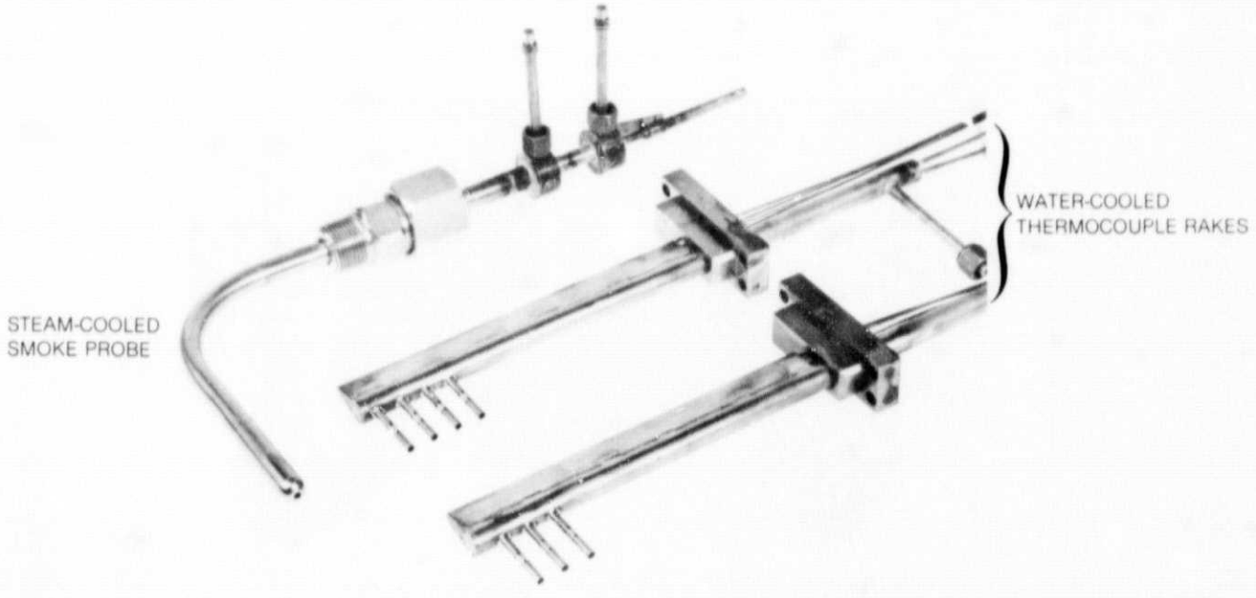

Fig. 11 Instrumentation at Combustor Exit

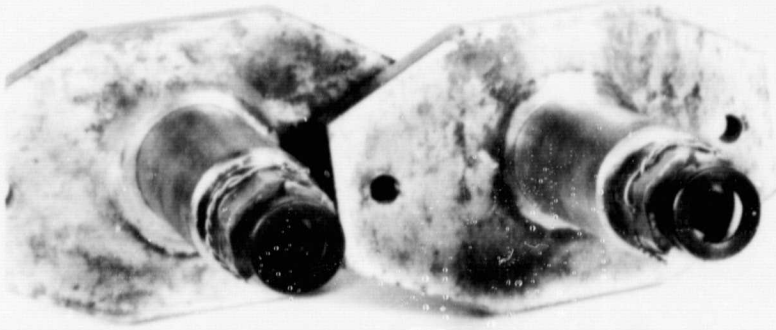

a. NON-SWIRL SHEATH

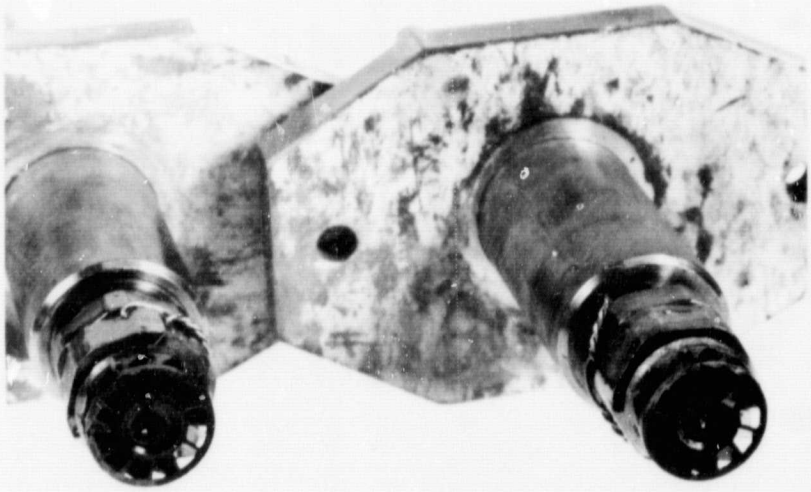

b. SWIRLER SHEATH

Fig. 12 Carbon Deposits on Spill Return Configurations

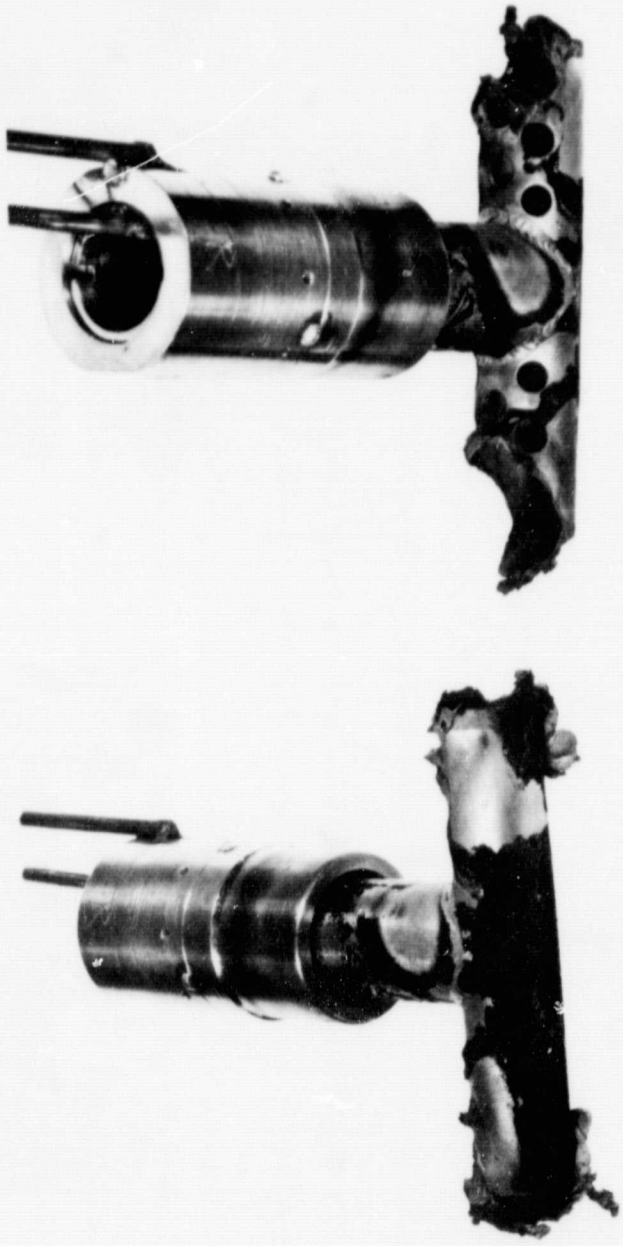

Fig. 13 Post-Test Condition of Bar Vaporizer

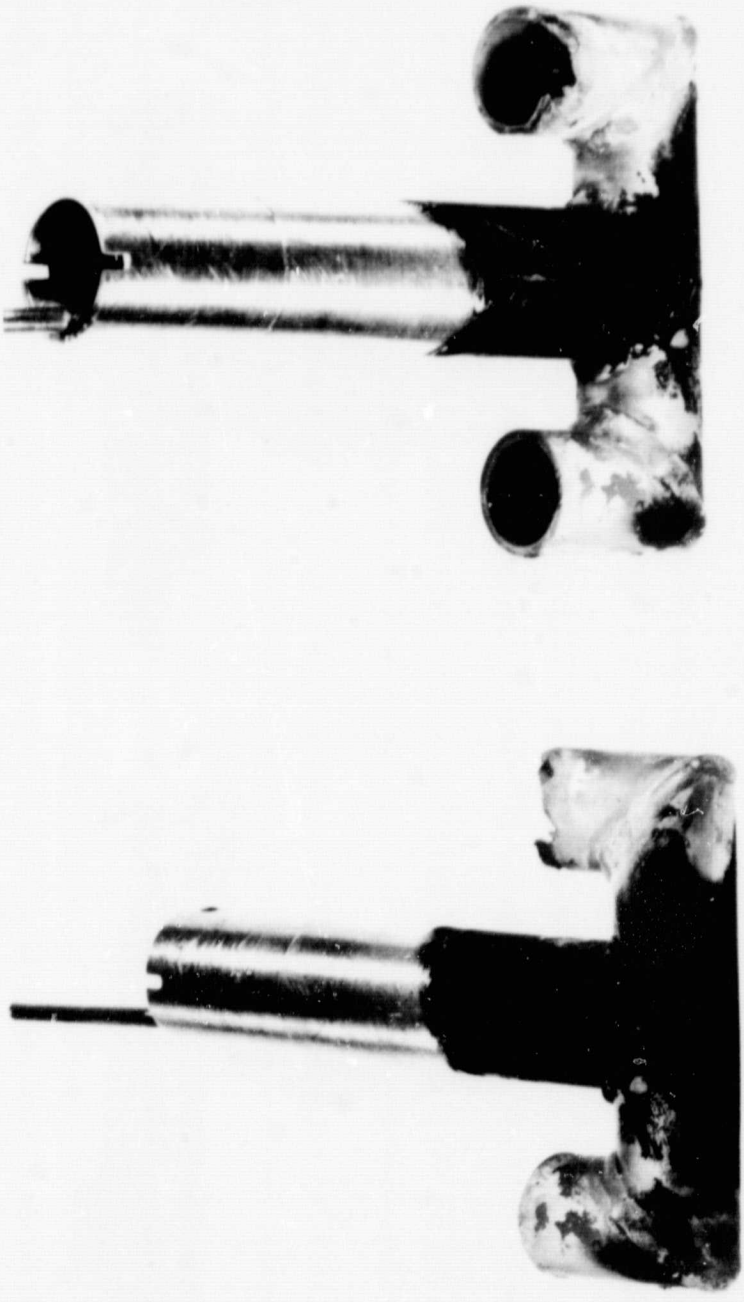

Fig. 14 Carbon Deposit on T-Vaporizer

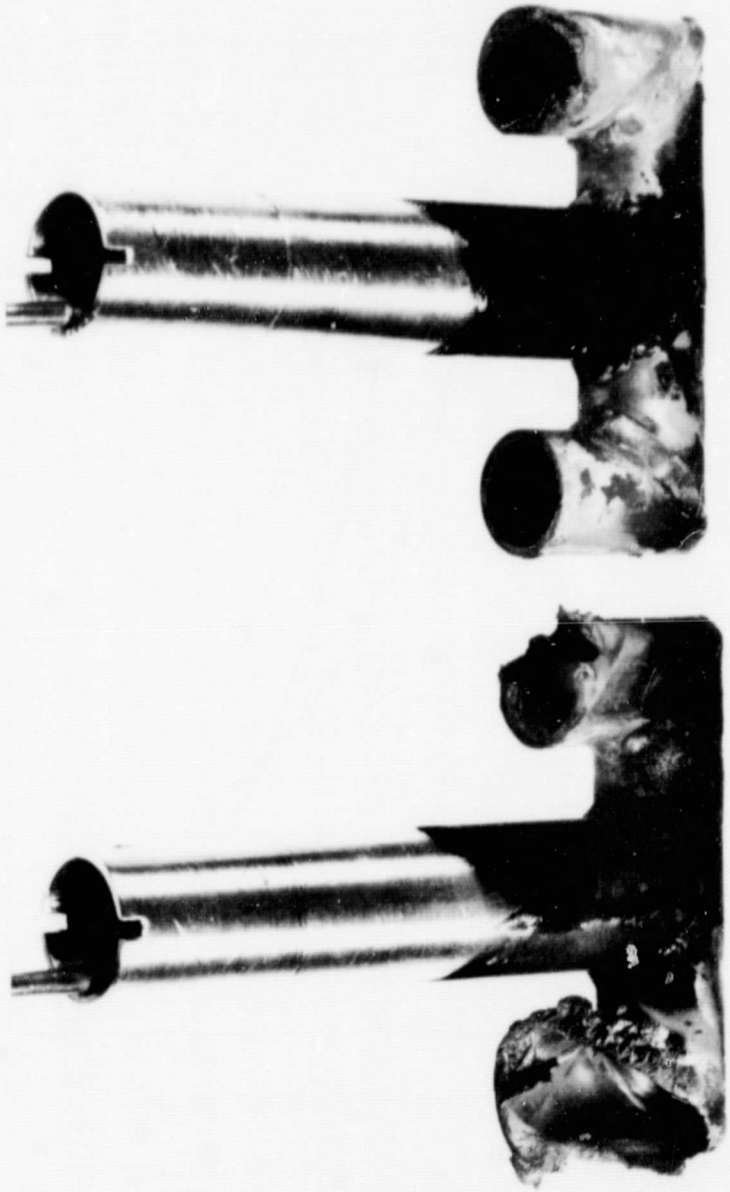

Fig. 15 Post-Test Condition of T-Vaporizer

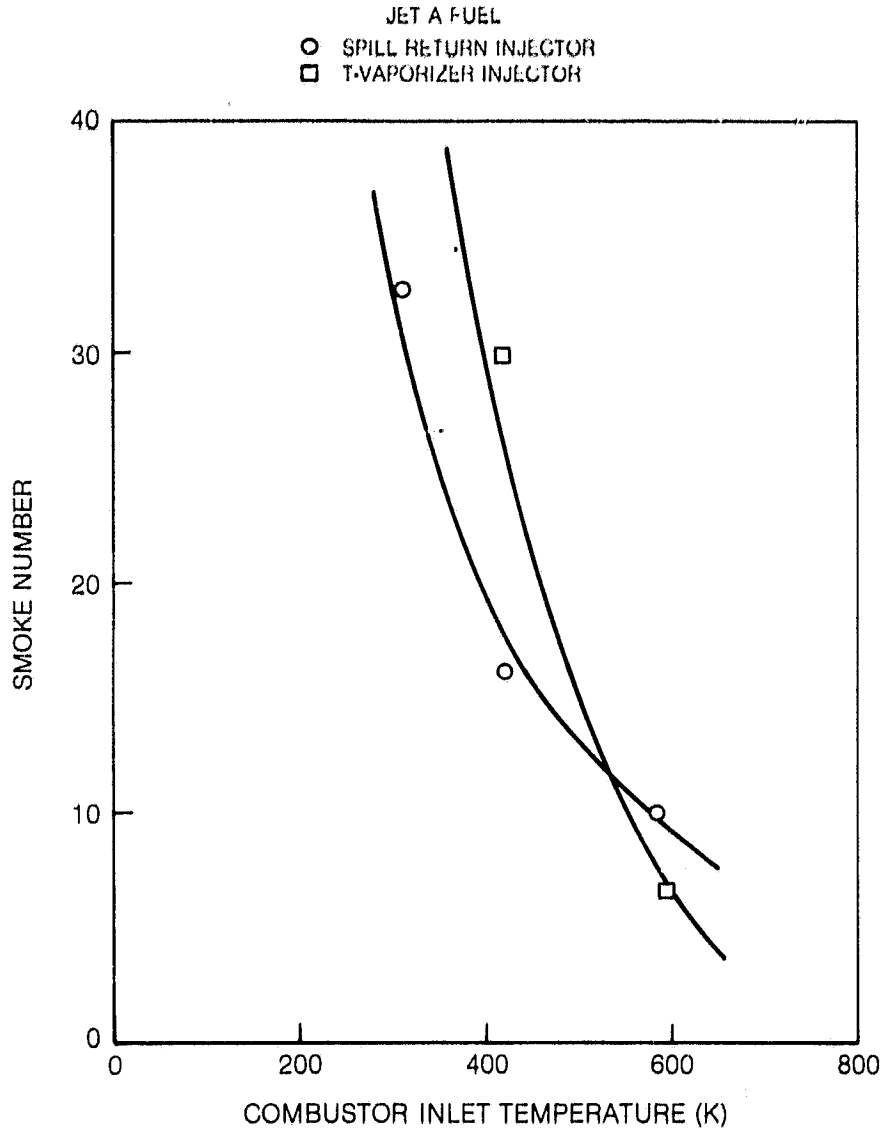

Fig. 16 Smoke Number Dependence on Inlet Air Temperature

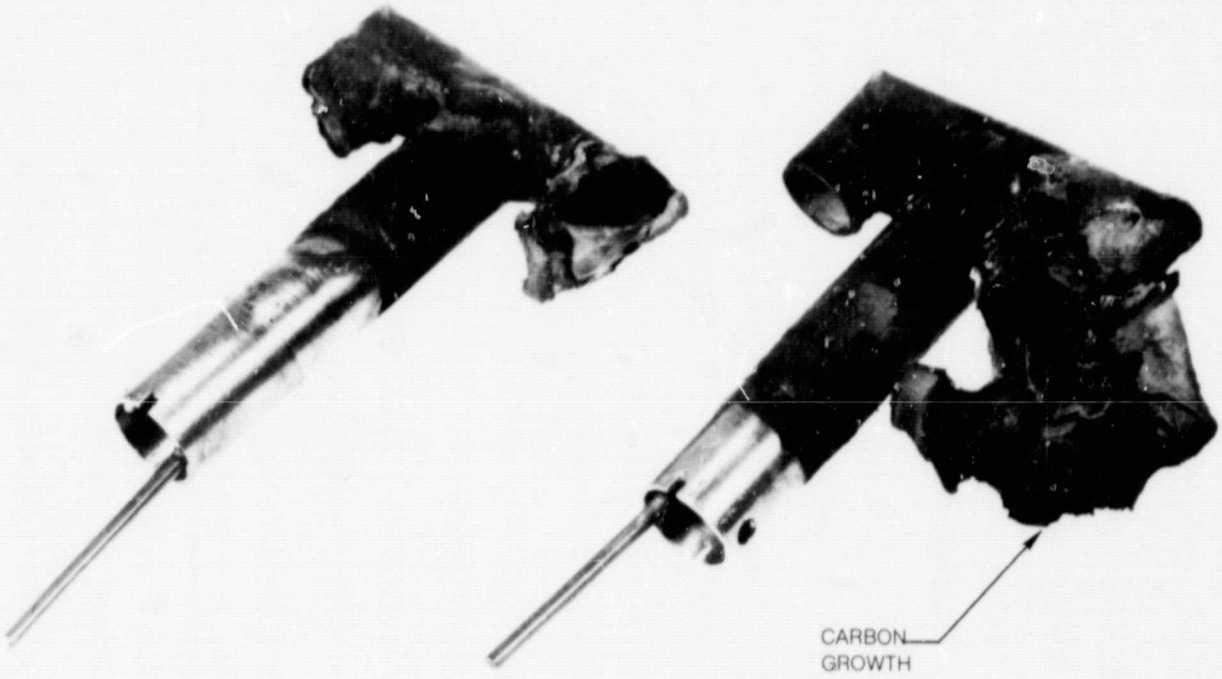

Fig. 17 Carbon Deposit Growth on T-Vaporizer After Operation at T3 = 300K

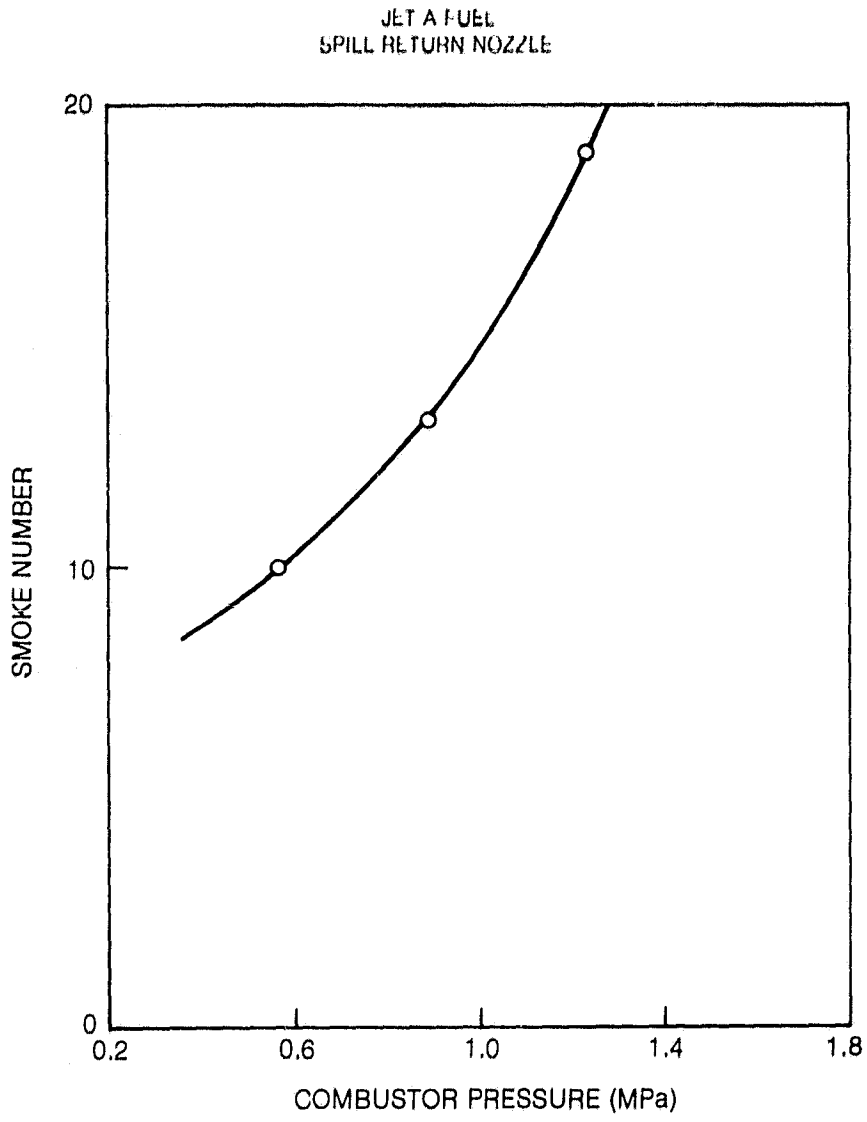

Fig. 18 Smoke Number Dependence on Combustor Pressure

82-2-28-9

JET A FUEL
SPILL RETURN NOZZLE

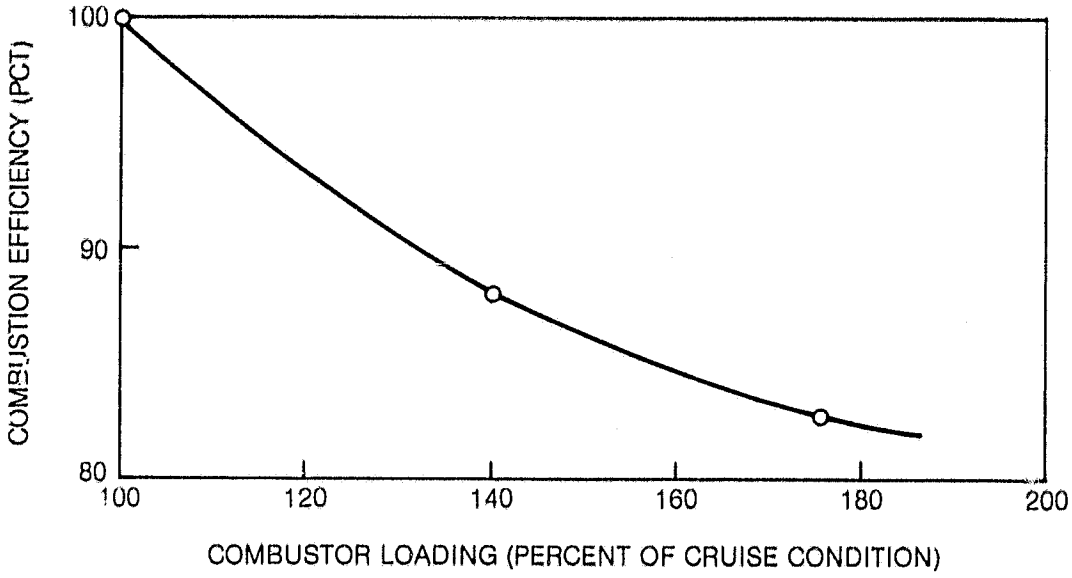

Fig. 19 Dependence of Combustion Efficiency with Combustor Loading